University of Helsinki

Faculty of Science

Department of Chemistry

Funded by the Erasmus+ Programme of the European Union

Erasmus Mundus Joint Master Degree "Advanced Spectroscopy in Chemistry"

MASTER THESIS

by

Elena Bandini

10-06-2019

Thermoresponsive microgels based on strong polycations

Research group: Polymers and Colloids

Supervisor: Erno Karjalainen

Reviewers: Erno Karjalainen, Sirkka Liisa Maunu

HELSINGIN YLIOPISTO
HELSINGFORS UNIVERSITET
UNIVERSITY OF HELSINKI

MATEMAATTIS-LUONNONTIETEELLINEN TIEDEKUNTA
MATEMATISK-NATURVETENSKAPLIGA FAKULTETEN
FACULTY OF SCIENCE

Tiedekunta – Fakultet – Faculty Faculty of Science	Koulutusohjelma – Utbildningsprogram – Degree programme Erasmus Mundus Joint Master Degree “Advanced Spectroscopy in Chemistry”

Tekijä – Författare – Author
Elena Bandini

Työn nimi – Arbetets titel – Title
Thermoresponsive microgels based on strong polycations

Työn laji – Arbetets art – Level Master	Aika – Datum – Month and year June 2019	Sivumäärä – Sidoantal – Number of pages 61

Tiivistelmä – Referat – Abstract

The aim of this work is to synthetize a series of thermoresponsive microgels that have never been reported before, based on strong polycations, and study their properties such as the change in volume in response to a temperature stimulus. Polymer microgels are interesting materials for practical applications as drug delivery systems, in separation techniques and catalysis. The interest on these materials arises from their physical properties of colloids combined with gel properties. The microgels presented in this work can undergo phase transitions not only in water but also in DMF/water mixtures. A crosslinked polymer that displays cloud point behaviour when heated forms a temperature-sensitive gel network. Cloud point is the temperature above which an aqueous solution of a water-soluble polymer becomes turbid in the case of polymer with LCST (Lower Critical Solution Temperature) behaviour. Upon heating such a gel, the gel shrinkage is observed by expelling water over a temperature range. The transition is largely driven by the entropy gain associated with the release of water from the network, and the concomitant collapse of the polymer chains. In addition, the size of the microgels is tuneable by adding NaCl at different concentration. The synthesis is carried out as a normal radical polymerization always in the same conditions except for the solvent mixture. The homopolymer, synthetized for comparison, is polymerized with RAFT (Reversible Addition-Fragmentation chain-Transfer) method. Nuclear Magnetic Resonance (NMR) confirmed the structure of the microgels validating the synthetic method. The hydrodynamic radius of the microgels after the addition of salty solutions at different concentration is determined by Dynamic Light Scattering (DLS). The thermo-responsive properties are investigated in terms of polarity using fluorescence and turbidity measurements and in terms of changes in volume calculated from the hydrodynamic radius with DLS at different temperature. The microgels show a thermo-responsive behaviour in the temperature range between 10 °C and 90 °C. In fact, the raise in temperature causes an increase in volume and hydrophobicity. Finally, it is reported a trend that follows the NaCl concentration of salt solutions added to the microgels.
These microgels can be used for a wide range of applications, amongst them, they are useful support for metal nanoparticles for catalytic purposes. Here, AuNPs are formed directly on the microgel and the formation is ascertained by DLS and TGA (Thermogravimetric Analysis). Then, they are tested to effectively work during a catalysis experiment.

Avainsanat – Nyckelord – Keywords
Acqueous polymers, LCST, stimuli-responsive polymers, thermoresponsive polymers, polymers, polyelectrolytes, counter ion, AuNPs, nanoparticles, microgels

Säilytyspaikka – Förvaringställe – Where deposited
University of Helsinki

Muita tietoja – Övriga uppgifter – Additional information

Contents

1 Introduction **4**

1.1 Thermoresponsive polyelectrolytes 4

1.1.1 Thermoresponsive polymers in water 5

1.1.2 The Hofmeister series 6

1.1.3 Polyelectrolyte effect 7

1.2 Thermoresponsive microgels 7

1.2.1 Polyelectrolyte microgels 8

1.2.2 PNIPAm 9

1.3 Synthesis 11

1.3.1 Radical Polymerization 11

1.3.2 RAFT 12

1.4 Characterization methods 14

1.4.1 Dynamic Light Scattering 14

1.4.2 Fluorescence Spectroscopy 15

1.4.3 Ultraviolet Spectroscopy 15

1.5 Applications 16

2 Experimental part **19**

2.1 Materials 19

2.2 Syntheses 19

2.2.1 [(4-vynilbenzyl)tributyl]ammonium chloride synthesis 19

2.2.2 Microgels synthesis 20

2.2.3 Homopolymer sythesis 21

2.3 Instrumentation and sample preparation 22

2.3.1 Nuclear Magnetic Resonance 22

2.3.2 Dynamic Light Scattering 22

2.3.3 Fluorescence spectroscopy 23

2.3.4 UV spectroscopy 23

2.4 Catalytic application 23

2.4.1 Preparation of the microgel-supported AuNP 23

2.4.2 Thermogravimetric analysis 24

2.4.3 Catalysis experiment 24

3 Results and discussion **25**

3.1 Polymerization process 25

3.2 Dynamic Light Scattering 26

3.3 Fluorescence 35

3.4 UV-spectroscopy 38

3.5 Microgel-supported AuNP 43

4 Conclusions **46**

Appendix **i**

Abbreviations and Symbols

4HP	4-(Dicyanomethylene)-2-methyl-6-(4-dimethylaminostyryl)-4H-pyran
ΔG	Change in Gibbs Free Energy
ΔH	Change in Entalphy
ΔS	Change in Entropy
η	Viscosity
ANS	8-Anilinonaphthalene-1-sulfonic acid
Cryo-TEM	Trasmission Electron Cryomicroscopy
CTA	Chain Transfer Agent
D	Self-diffusion coefficient
DLS	Dynamic Light Scattering
DMF	Dimethyl formamide
IL	Ionic Liquid
k	Boltzmann constant
LCST	Lower Critical Solution Temperature
NMR	Nuclear Magnetic Resonance
PIL	Poly(Ionic Liquid)
PNIPAm	Poly(N-isopropyl acrylamide)
RAFT	Reversible Addition Fragmentation chain Transfer
R_h	Hydrodynamic Radius
T	Temperature
T_c	Cloud point Temperature
TGA	Thermogravimetric Analysis
UCST	Upper Critical Solution Temperature
UV	UltraViolet
VBA	[(4-Vinylbenzyl)trialkyl]ammonium

1 Introduction

This work is a study of the stimuli-responsive volume phase transitions of a class of polyionic liquid microgels. These microgels are synthesized with small amounts of a crosslinker, so that they can undergo volume phase transition in response to the changes in temperature in water or water/DMF mixture.

1.1 Thermoresponsive polyelectrolytes

Recently, the research has been more focused on a new class of polymers which change their physical and/or chemical properties in response of an external stimulus. Stimuli-responsive polymers, also called smart or intelligent polymers are synthetized to be reactive at different stimuli like pH, temperature, mechanical force, the presence of various small molecules and biomolecules, and electric/magnetic fields.[1] The most well-studied are the ones that respond to changes in temperature, named thermoresponsive polymers, because temperature plays an important role in nature, it can be externally applied in a non-invasive manner and the behaviour is often completely reversible.[2] In addition, multi-responsive polymers can be synthesized by incorporating other functional groups into the temperature responsive polymer.

These polymers have found applications in many fields, for example in medicine as sensing and biosensing, controlled drug delivery systems, artifical muscles and actuators, as well as in catalysis, separation techniques, coatings and textiles, polymer electrolytes, carbon precursors and fuel cell membranes.[1,3,4]

The polymers synthetized in this work are poly(ionic liquids) also referred as PILs, they are a class of polyelectrolytes that have as monomeric repeating unit ionic liquid (IL) species. Polyelectrolytes are polymers with charged groups attached to their backbone and consequently an equivalent amount of opposite charges. They can be classified into anionic, cationic and zwitterionic polyelectrolytes depending on the type of charge. ILs are salts that are liquid at ambient temperature, as a definition their melting point is lower than 100° C. They consist of an organic cation and an organic or inorganic anion. ILs show extremely interesting properties such as chemical, thermal and electrochemical stability, high electric conductivity, high thermal capacity, moreover they are not flammable and good solvents.[5] These properties can be tuned changing the anion.

Generally, the same anions bring similar properties to ILs and PILs. The counter ion responsivity is a characteristic of PILs in the meaning that the choice of the counter ion influences many properties of the PILs such as solubility, glass transition temperature and thermal stability.[4]

PIL colloids are very interesting because they combine the unique properties of ILs with the small dimension and the superior dispersity of colloidal particles.[6]

1.1.1 Thermoresponsive polymers in water

When polyelectrolyte dissolves into water, all or some of the functional groups are ionised and counter ions are released into the solution, leading to a certain conformation of the polyion, globular, rod or coil state, depending on the polymer-polymer and polymer-solvent interactions.[2] When most of the groups are ionized the conformation of the polymer backbone is more stretched and it is referred as a coiled conformation. On the other hand, in case of a dominant hydrophobicity, the polyelectrolyte is referred to have a globular conformation.

There are two main types of temperature responsiveness in water as well as in other solvents. One is named LCST which stands for polymers with a Lower Critical Solution Temperature. It means that the elevation of temperature leads to the formation of two immiscible phases with different polymer concentration. The temperature of the minimum of the binodal of the phase diagram define the LCST.[2] A large number of polymers have been demonstrated to have measurable LCST transitions under standard conditions. The other type of temperature responsiveness is UCST behaviour (Upper Critical Solution Temperature) which means that the phase separation happens upon cooling. These polymers are typically hydrophilic species, insoluble below a critical temperature because of strongly attractive polymer−polymer interactions that are broken by water. They are much less frequent.[7–9] Nonionic homopolymers with UCST behaviour in liquid water often contain primary amine groups. Polyelectrolytes with UCST are polymers with zwitterionic groups for example. Cloud point temperature is usually dependent on concentration and additives such as electrolytes. Higher ionic strenght shows increased solubility. It is also possible to induce a UCST type of transition to a weak polycation in a suitable pH range by the introduction of a multivalent counter ion.[10]

The sudden change in hydrophobicity of the polymer is based on hydrogen bonds between the polymer and surrounding water molecules. The polymer chains are hydrated and solubilized in the one-phase system. In the LCST case, increasing temperature, the hydrogen bonds are weakened and the polymer chains are partially dehydrated. As a consequence, the polymer is no more soluble and it aggregates. This phase transition is entropy-driven. It derives from the the Gibbs free energy $\Delta G = \Delta H - T\Delta S$, at high temperature $T\Delta S$ is predominant and the free energy turns positive, because the binding of water molecule to polymer chains leads to ΔH, the enthalpy term, always favorable and ΔS is always negative in the case of LCST behaviour. This is manifested in phase separation.[2,11] When the polymer precipitates it is the other way around. For example, heating PNIPAm (poly(N-isopropyl acrylamide)) leads to a strong endothermic transition and the enthalpy is unfavourable. According to the study conducted by Idziak et al.[11] the addition of sodium chloride to the polymer solution results in a linear decrease of the LCST.

1.1.2 The Hofmeister series

The ability of salts to precipitate or dissolve proteins from an acqueous solution follows a recurring trend known as Hofmeister series. Anions appear to have a larger effect than cations, here following their order:[12]

$CO_3{}^{2-} > SO_4{}^{2-} > S_2O_3{}^{2}- > H_2PO_4{}^{-} > F^{-} > Cl^{-} > Br^{-} \approx NO_3{}^{-} > I^{-} > ClO_4{}^{-} > SCN^{-}$

The typical order for cations is:

$NH_4{}^{+} > K^{+} > Na^{+} > Li^{+} > Mg^{2+} > Ca^{2+}$

The species on the left are referred to as kosmotropes and the ones on the right as chaotropes. In the case of a thermo-responsive polymer this series can be explained on the basis of direct interactions of the ions with the macromolecule and its hydration shell. Even though the phase transition mechanism is different for kosmotropes and chaotropes.[13]

In the case of a polyelectrolyte, the LCST behaviour can be modulated by the counter ion.[14] The salt effects on the LCST of PNIPAm have been reported and related to the Hofmeister series. PNIPAm bears both hydrophilic (amide) and hydrophobic (isopropyl) groups, as a consequence it works as a model system for cold denaturation

of peptides and proteins. Three interactions give the explanation of the effects of Hofmeister series on PNIPAm solvation. First, the anions can polarize an adjacent water molecule involved in hydrogen bonding with the amide. Second, the salt can interfer with the hydrophobic hydration of the macromolecule by increasing the surface tension of the cavity surrounding the backbone and the isopropyl chains. These two effects lead to salting-out of the polymer, they lower the LCST. The last effect is that the anions may bind directly to the polyamide, which leads to the salting-in of the polymer and an increase in LCST.[12,13]

1.1.3 Polyelectrolyte effect

The counter ions that surround a polyelectrolyte dissolved in an acqueous solution can behave in different ways, some of them stay attached to the backbone, others are completely free in the solution and others are free in solution but feel the attraction to the opposite charges. When small amount of salt is added to the polyelectrolyte solution, the ions attracted to the polyions screen the charges of the ionised groups. As a consequence the polymer collapse into a coil and the viscosity decreases (Fig. 1). This reduced viscosity of polyelectrolyte solutions as the solution is diluted is completely different from the behaviour of neutral polymers.[15,16] We can refer to "polyelectrolyte effect" when the reduced viscosity of a polyelectrolyte increases upon dilution, it results from the intra-molecular electrostatic repulsion. This abnormal behaviours can be ascribed to interface effect.[17]

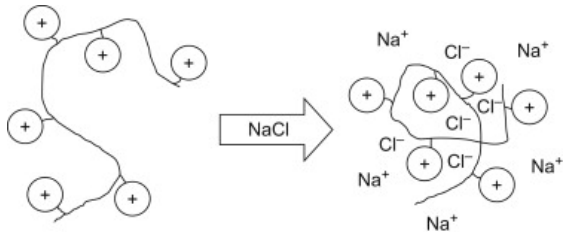

Figure 1. Polyelectrolyte effect.

1.2 Thermoresponsive microgels

In this study case we deal with microgels, that means that the particles have microscale size (50 nm to 10 μm). Microgels can be defined as intramolecurarly crosslinked, high

molecular weight, soluble polymers.[18] These particles are crosslinked polymer chains stable in acqueous solutions thanks to electrostatic and sterical interaction, due to the attached charged groups which interact with each other giving rise to both the interactions mentioned.[19] In microgels the polymer chains are significantly swollen by the solvent.[6] Aqueous microgel particles with small dimensions present a unique class of nano-objects. Because of the crosslinked state, the interior is discriminated from the surface groups in accessability but also in chemical reactivity. Because of the hydrophilic nature of the constituent segments, nanoparticulate hydrogels are colloidally stable in water without need of adding surfactant molecules. The gel shape is preserved thanks to the covalent crosslinking.[6] Moreover, because of their water solubility and water uptake, the microgel particles can take part in short- and long-range interactions. Thanks to the small size and the large surface to volume ratio, the swelling/deswelling response to a change in temperature is nearly instantaneously compared to macrogels.[20] The advantage of these polymer gels is that they are like solid materials with the fluidity of a liquid at the microscale level.[21–23]

Polymer microgels are interesting materials for practical applications as drug delivery systems, in separation techniques and catalysis.[24–30] This interest arises from their physical properties of colloids combined with gels properties. They show both properties of solid and fluid, which leads to advantages such as dispersible, high intrerface area per unit mass, great exchange rate, fast kinetics in repsonse to changes and suitable size for microscale uses.[31–37] Thermoresponsive microgels are sensitive to temperature changes, they enable the fabrication of stimuli-responsive materials.[20] Thermosresposive microgels show also a cloud point temperature (T_c) which correnspponds to the temperature when the polymer solution starts to phase-spearate at a specific concentration, to the collapsed aggregated state, visible as clouding of the solution. Hence it is possible to observe two phases and an increase in turbidity. The LCST is the lowest value of T_c in the phase diagram. The T_c of a polymer can be easily varied by copolymerization or end-group modification to tune the hydrophobicity of the polymer.[2]

1.2.1 Polyelectrolyte microgels

Acqueous microgels have attracted considerable interest as building blocks for advanced functional materials due to their responsiveness to external stimuli like pH and temper-

ature, their ability to retain water, or the possibility to entrap large amounts of guest molecules in the gel network for controlled release applications. The ability to manipulate the chemical structure and to develop microgels with new solution properties, is crucial for the broadening and advancing of the applications.[38,39]

Polyelectrolytes can be divided into two groups, weak and strong polyelectrolytes, showing ionization behaviour with and without pH-dependence respectively. The incorporation of these ionic groups into classical microgels synthesis can lead to new microgels with better properties.[38]

Most often, charged comonomers are incorporated into microgels.The addition of small amount of comonomer can have a dramatic effect on the overall properties of the resultant microgel particles.[40] These polyelectrolyte microgels that are formed can carry either positively or negatively charged comonomers but they can also be polyampholyte microgels. The addition of oppositely charged molecules to charged microgels leads to a strong interaction within the microgels and allows modification of the properties such as the size or the electrophoretic mobility. The complexes show no tendency to flocculate when the electromobility is neutral, contrary to complexes of rigid nanoparticles and polyelectrolytes. The interaction between polyelectrolytes and microgels is mainly driven by electrostatics, non-specific interactions exist.[41]

1.2.2 PNIPAm

One of the most studied polymers that shows LCST behaviour is poly(N-isopropylacrylamide), PNIPAm (Fig. 2). It exhibits a LCST at 32°C. As the solution temperature rises above the LCST, PNIPAm chains undergo a transition from an extended and solvated random coil to a compact and desolvated globular conformation known as mesoglobules, depending on the concentration.[42,43] In very dilute solutions, the globules are stable, but a higher concentration leads to the formation of stable mesoglobules.[44] The coil-to-globule transition can be observed as a decrease in the hydrodynamic radius. For individual polymer chains, the coil-to-globule transition can be thermodynamically controlled by adjusting the polymer composition, the LCST shift to higher or lower temperature for example by copolymerization with a hydrophilic or hydrophobic monomer.[1]

Low concentration of salts increases the cloud point temperature due to the interactions between the anions of the salt and the amide groups of the polymer and changes in sur-

face tension around the hydrophobic groups.[12,13] At the cloud point, the polymer chains dehydrate and new intra- and intermolecular hydrogen bonds are formed. In particular, the breaking of the hydrogen layer around the isopropyl groups plays a central role. Even above the T_c, the polymer globules are still hydrated and a large majority of the amide groups keep hydrogen bonded to water.[44]

Typically, the surface tension of PNIPAm solution decreases significantly with temperature, as a consequence we have increased adsorption to the interface below the phase transition temperature. When the phase transition temperature is reached, the surface tension remains constant and the collapsed PNIPAm aggregates remain adsorbed to the interface.[42]

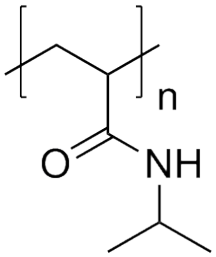

Figure 2. PNIPAm structure.

A linear polymer that displays cloud point behaviour when heated can be crosslinked to give a temperature-sensitive gel network. Upon heating such a gel, one observes the gel to shrink by expelling water over a narrow temperature range.[33] The cloud point is the temperature above which an aqueous solution of a water-soluble polymer becomes turbid in the case of polymer with LCST behaviour. Upon heating such a gel, the gel shrink is observed by expelling water over a temperature range. The transition is largely driven by the entropy gain associated with the release of water from the network, and the concomitant collapse of the polymer chains. In hydrogel or microgel form, this thermoresponsivity is manifest as a thermoinduced volume change arising from the dramatic expulsion of water as the temperature is raised.[36] The network undergoes a volume collapse at the temperature, as opposed to the nearly complete desolvation observed in the case of linear homopolymer. Chemically crosslinked PNIPAm microgels reveal a drastic particle size decrease upon heating in aqueous solution. The responsive characteristics can be modified by either co-polymerization or advanced polymer architecture.[45]

Tanaka et al. noticed that PNIPAm solutions in the mixed solvent of water and methanol shown a sharp depression of cloud point.[46] This phenomenon is one of the three cases studied of polymers behaviour in mixed solvents. If we have a combination of two solvents that are poor solvents for the polymer but good when mixed we are in the case of cosolvency. The opposite situation, two good solvents for a polymer that become poor when mixed, is called co-nonsolvency. The last case is when the two solvents are a nearly incompatible mixture, the polymer collapses due to the concentration fluctuation of the solvent mixture, followed by the reswelling to the ideal state.
The PNIPAm behaviour can be ascribed to the co-nonsolvency phenomena in the case of methanol-mixture as a solvent. There are three theories to elucidate the PNIPAm co-nonsolvency. The first one postulates that the main cause is the formation of a H-bonding network between water and methanol molecules. The second one stresses the cause on the preferential adsorption of one component near the polymer chain which induces attractive interaction between the chain segments. Finally, the last interpretation is the selective adsorption by competitive H-bonding.[46]

1.3 Synthesis

The microgles are synthetized with radical polymerization method while the homopolymer synthetized from the same monomer as the microgels but without the crosslinker, is synthetized following a RAFT (Reversible Addition-Fragmentation chain Transfer) polymerization.

1.3.1 Radical Polymerization

Radical polymerization involves the formation of free radicals via decomposition of an initiator by light, electromagnetic radiation like γ radiation, temperature, or redox reaction. The formed free radicals react consequently with the monomer leading to the formation of a polymer network. It remains one of the most important industrial technology for the production of vinyl-based polymeric materials due to its versatility and synthetic ease[47]
There are four basic reaction steps (Fig. 3):

- Initiation

- Propagation
- Chain transfer
- Termination

The initiation step involves the generation of reactive free-radicals followed by the addition of a monomer molecule to form chain radicals. The chain radicals propagate by the addition of monomer molecules to form long polymer chains. Then we can have chain transfer by abstraction of hydrogen from the small molecule by the chain radical. This leads to termination of the chain. At the same time, a new primary transfer radical is formed which can start chain polymerization. There are two mechanism to terminate the polymerization, combination and disproportion. In termination by combination, two living polymer end groups react with each other, forming a single dead chain. In disproportionation reaction, the radical at the end of one chain attacks a hydrogen atom at the second-to-penultimate carbon atom in the second chain, forming two dead polymer molecules with no net change in molecular weight.[47]

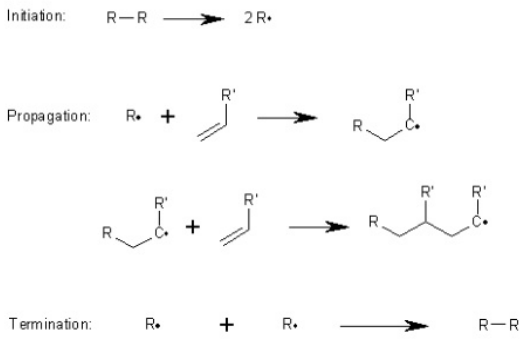

Figure 3. Free radical polymerization mechanism.

1.3.2 RAFT

The main methods to perform controlled radical polymerization are Atom Transfer Radical Polymerization (ATPR) and Reversible Addition-Fragmentation chain Transfer (RAFT), they allow the synthesis of homopolymer and copolymers with different architectures and narrow molecular weight distributions.[48]

RAFT is based on degenerative chain transfer. It is initiated as a normal radical polymerization then the intermediate radical can fragment either back towards the polymeric

radical or liberate a re-initiating radical, in the latter case a new polymer chain is created. This method is controlled by a chain transfer agent (CTA) which slows down the chain growth.

The mechanism (Fig. 4) starts with a radical initiator that decomposes in two fragments that react with the monomer molecules. The propagating chain then adds the CTA with a fragmentation reaction, the newly created radical can release the original growing radical or a new initiating species. When all the CTA is consumed an equilibrium is established between active and dormant states. This equilibrium is the key to have narrow polydispersity because it allows equal probability for all the chains to grow. At the end we have the termination, which is suppressed in the case of RAFT because chains in their active form react bi-radical termination to form chains that cannot react further, called dead polymers.[49]

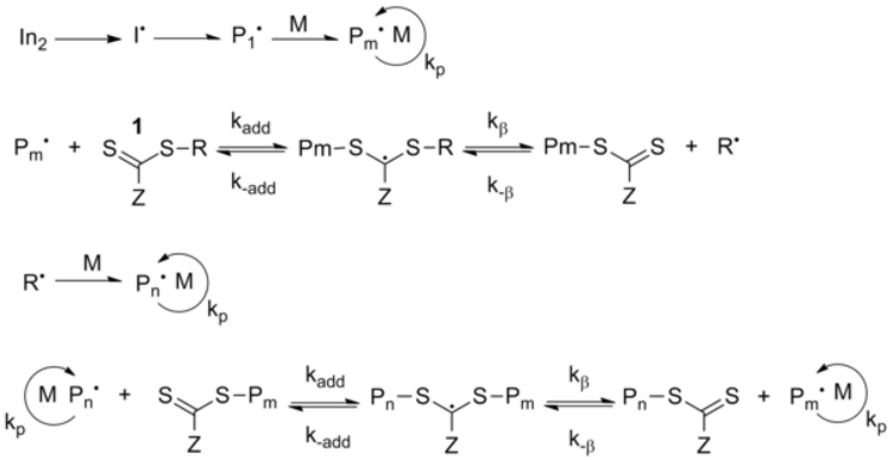

Figure 4. RAFT mechanism.

Ideally, the RAFT adduct radical is sufficiently hindered that it doesn't undergo termination reactions. CTA's agents are usually thiocarbonylthio compounds such as dithioesters or trithiocarbonates (Fig. 5).[50]

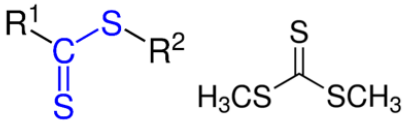

Figure 5. Dithioester and trithiocarbonate structures.

1.4 Characterization methods

The microgels structure are confirmed by NMR (Nuclear Magnetic Resonance). The heating or cooling of thermoresponsive materials leads to various and drastic changes in physical and chemical properties of the polymer when crossing the phase transition temperature, such as chain conformation and mobility, hydrogen bonding, and optical properties that can be tested with different techniques.[2] In this work dynamic light scattering, fluorenscence and UV spectroscopy are used.

1.4.1 Dynamic Light Scattering

Dynamic Light Scattering (DLS) is a spectroscopic technique that arises from fluctuations in scattered intensity of scattered particles moving following a Brownian motion.[15] Experiments using light as a probe offer information on the size, shape, and interactions of macromolecules.[51]

The instrumentation consists in a laser to produce high intensity monochromatic light, in this case blue laser, λ = 488 nm, which is adjusted by mirrors and modulators and focused on a sample solution that contains the polymer. A detector is placed in a goniometer to measure the intensity of the scattered light at many different angles (Fig. 6). The pinhole in front of the detector is 2 mm. The scattered intensity from very short time intervals, is recorded as a function of time. The detector transforms the signal into an electronic signal which can be described by its autocorrelation function. The autocorrelation function of the scattered intensity is the convolution of the intensity signal as a function of time with itself. The DLS provides measurements of the hydrodynamic radius (R_h) of the synthetized microgel. In this work it is used to study the changes in radius of the particles at different salt concentration. The DLS measures the self-diffusion coefficient (D) which is correlated with the size of the particles according to the Stokes-Einstein equation $R_h = kT/(3\pi\eta D)$, where k is the Boltzman constant, T the temperature in Kelvin and η the viscosity of the dispersing medium.[2] The zetasizer instrument is also used to measure the particle size. The system determines the size by measuring the Brownian motion of the particles in a sample using DLS mode. It detects the scattering information at 175° angle (backscattered detection).

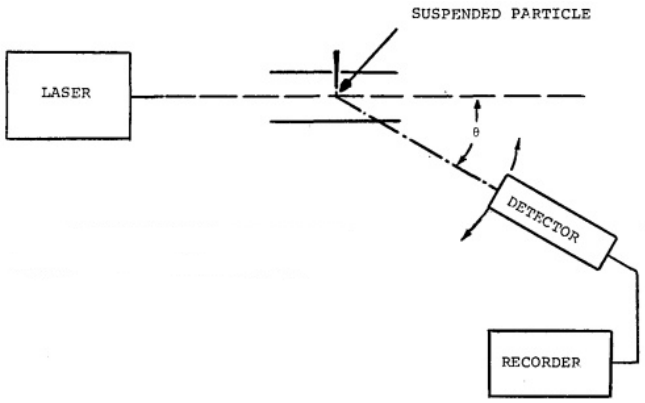

Figure 6. Light scattering instrumentation.

1.4.2 Fluorescence Spectroscopy

Fluorescence spectroscopy is used to study aggregation, micellization and micropolarity of micelles and mesoglobules.[42] It is used to elucidate conformational changes occurring along the microgel backbone. Additionally, the thermodynamic properties of a polymer over the course of a varying temperature scan provide important information regarding its thermal stability.

Fluorophores are used as probe. Pyrene yields informations about the polarity around it. 4-(Dicyanomethylene)-2-methyl-6-(4-dimethylaminostyryl)-4H-pyran (4HP) is a probe that can be used to study the mobility and rigidity (microviscosity) of its immediate surroundings. 4HP emits very weakly in water but is known to emit strongly in micellar systems. Higher intensity corresponds to higher viscosity.[42]

1.4.3 Ultraviolet Spectroscopy

A UV-visible spectrophotometer, coupled to a temperature controller is used to optically measure the cloud point temperature. The LCST is defined as the temperature at which the differential of transmittance with respect to the temperature at a certain wavelength is maximal.[11] The wavelength of the measurement determines the minimum size of precipitated particles detected.[51]

The spectrophotometer is composed of a source of light, a monochromator, a detector and a recorder (Fig. 7).

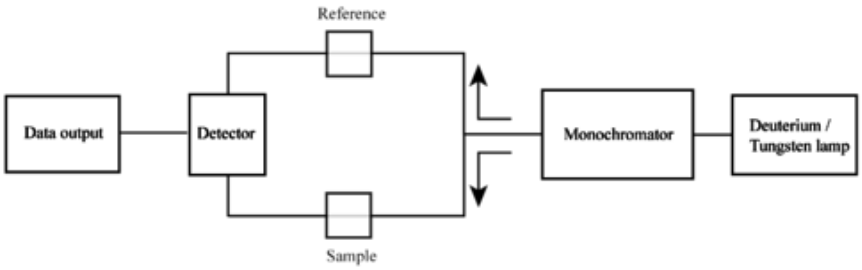

Figure 7. UV spectrometer.

1.5 Applications

Amongst the many possible applications, here the microgels are tested as nanoparticles stabilizer.

Metal nanoparticels show different properties as compared to their bulk materials. Due to their high surface-to-volume ratio, metal nanoparticles of noble metals are ideally suited for catalysis.[52–56]

Gold nanoparticles (AuNPs) present interesting aspects such as their assembly of multiple types involving material science, the behaviour of the individual particles, size-related electronic, magnetic and optical properties, and their application to catalysis and biology. Gold is very popular for being chemically inert. It is one of the most stable metals in the group 8 elements and it is resistent to oxidation. Catalysis with AuNPs, in particular the very active oxide-supported ones, is now an expanding area, and a large number of new catalytic systems for various reactions are now being explored.[57] However, such nanoparticles require a suitable support to prevent flocculation during the reaction to be catalyzed. For applications taking places at low temperature and in an acqueous environment, polymers, dedrimers, microgels and colloids are optimal carrier systems, they bind to metal clusters and prevent aggregation of the particles into bulk materials.[55] Since the support should be totally inert, in order to provide a quantitative analysis, no stabilizing agent should be induced that may alter or block the surface of the nanoparticles. However, the support should be sufficiently stable to ensure the reuse of the catalyst after the reaction. Another problem is the formation of well-defined nanoparticles with a narrow size distribution that should take place directly on the support.[58,59]

The AuNPs are generated in salt-free solutions, where the counter ions are strongly con-

fined within the charged layer attached to the surface of the core particles. The counter ions derived from the synthesis can be replaced by suitable ions of noble metals. Subsequent reduction of the metal ions nanoparticles can be achieved by suitable reagents such as $NaBH_4$. The advantages of this method are that the nanoparticles are confined on the colloidal carrier and no additional stabilizing agent is needed to keep the metal particles in the truly nanoscopic range.[52]

To ascertain the method, different analytical techniques can be used. In this case, the size of the microgels loaded with AuNPs is measured by DLS. The total amount of gold is determined by thermogravimetric analysis (TGA) and cryo-TEM is used to veritfy the particles in situ.

As a model reaction for the catalytic activity, it is used the reduction of 4-nitrophenol by $NaBH_4$. Using an excess in concentration of $NaBH_4$ the kinetics of reduction can be treated as pseudo-first-order. Morever, the large excess of $NaBH_4$ takes into account the hydrolysis of this reagent at pH 10. The process of reduction can be monitored by UV-vis spectroscopy at different time. In figure 8 is shown the typical UV-vis spectra for the reduction of 4-nitrophenol measured at different time. 4-nitrophenol shows a characteristic peak at 400 nm, which decreases with time, while a new peak at 290 nm appears due to the formation of 4-aminophenol.[52] From the decrease of the peak at 400 nm it is possible to derive the rate constant. The apparent rate constant (k_{app}) can be obtained from the curve of $\ln(c_t/c_0)$ versus time by linear fit.[55]

This study is fascinating also from the point of view of the pollution abatament. Indeed water is polluted by phenol and phenolic compounds, among them, nitrophenols are some of the most refractory pollutants that can occur in industrial wastewater. More particurarly, nitrophenols and their derivates result from the production processes of pesticides, herbicides, insecticides and synthetic dyes. Moreover, the product, 4-aminophenol, is used as corrosion inhibitor, photographic developer, drying agent and important precursor or intermediate for preparation of drugs and chemicals.[56,58]

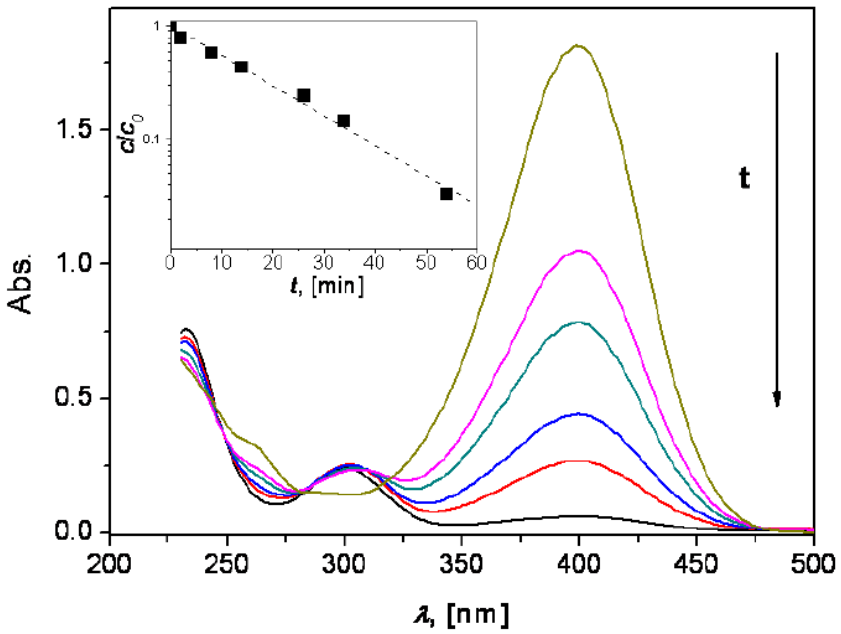

Figure 8. UV-vis kinetic curve of the reduction of 4-nitrophenol, and first order plot.[55]

2 Experimental part

2.1 Materials

2,6-di-tert-butyl-4-methyl phenol (Aldrich), 4-vinylbenzyl chloride (Aldrich, 90%), tributylamine (Fluka, puriss. p. a. $\geq$99.0% GC), acetone (Aldrich, HPLC grade 99.8%), diethyl ether (VWR, 100%), distilled water, NaCl (Fischer, an. reag. grade 99.98%), $NaNO_3$ (VWR, 99%), MeOD (99.8%), 1,4-dibromobutane, vinylimidazole, 2,6-di-tertbutylphenol, 2,2'-azobis(2-methylpropionitrile), 2-cyano-2-propylbenzodothionate, $HAuCl_4$, $NaBH_4$, 4-nitrophenol are used as received. N,N-dimethylformamide (Fluka, HPLC grade, purum. >99%) is distilled under reduced pressure. N,N'-methylenebisacrylamide (Aldrich, 90%) is recrystallized from acetone and water. 2,2'-azobis[2-(2-imidazolin-2-yl)propane]dihydrochloride is recrystallized from methanol.

2.2 Syntheses

2.2.1 [(4-vynilbenzyl)tributyl]ammonium chloride synthesis

Chemical	Mass	Quantity
4-vinylbenzyl chloride	10.0031 g	0.066 mol
tributylamine	12.1582 g	0.066 mol
2,6-di-tert-butyl-4-methyl phenol	100.65 mg	0.457 mmol
acetone	10 mL	

Table 1. Quantities of the chemicals for the monomer synthesis.

The reagents together with the inibithor and the solvent (Tab.1) are transferred in a flask and put under nitrogen flux for 10 minutes. The flask is then placed in an oil bath at 40°C to start the reaction which is carried out for 24 hours. The product is precipitated with diethyl ether, filtered with a paper filter and dried under vacuum for two hours. Then stored in the freezer. The characterization is carried out by NMR in MeOD.

2.2.2 Microgels synthesis

N,N´-methylenbisacrylamide is recrystallized from acetone and water and freezed. 2,2'-azobis[2-(2-imidazolin-2-yl)propane]dihydrochloride is recrystallized from methanol. Solutions with different concentration of salt (Tab. 2) and solutions with different percentage of N,N-Dimethylformamide (DMF) in water (Tab. 3) are prepared. In one flask is placed the monomer and the crosslinker together with 48 mL of the solution and in another the initiator with 2 mL of the solution (Tab. 4).

The two flasks are put under nitrogen flux for 45 minutes. After that, the flask containing the monomer is placed in an oil bath at 80°C for few minutes, still under nitrogen flux, then the initiator is added using a nitrogen flushed syringe and the nitrogen flux is stopped. The reaction is carried out for 2 hours with stirring rate of 500 rpm. The product is characterized by NMR with MeOD and stored in the fridge.

Concentration (M)	**H_2O (mL)**	**NaCl (g)**
1.5	100	8.766
1	100	5.844
0.75	100	4.383

Table 2. NaCl concentrations used for the microgels synthesis.

H_2O %	**DMF %**
70	30
50	50
30	70
10	90

Table 3. H_2O/DMF percentage values.

In the same way others two microgels with different paramenters are synthesized. Both the microgels are synthesized in the solution made of DMF/H_2O with 50% mixing. One of them is with a lower percentage of crosslinker (2%). Another one is synthesized using a different crosslinker. The crosslinker is synthesized following the reaction

Monomer concentration (M)	Monomer (mol)	Crosslinker (%)	Initiator (%)	Solution (mL)
0.1	0.005	5	1	50

Table 4. Molar percentages of the chemicals used for the synthesis of the microgels.

shown in figure 9.

The reagents (Tab. 5) are placed in a flask under N_2 flux for 30 minutes, then moved in an oil bath at 50°C overnight. The product is precipitated in EtOAc and stored in a freezer.

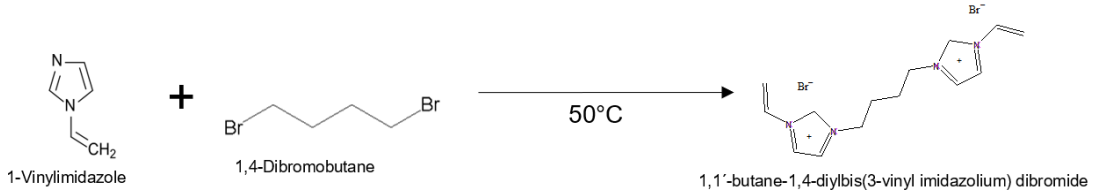

Figure 9. 1,1´-butane-1,4-diylbis(3-vinyl imidazolium) dibromide synthesis.

Chemical	Quantity (mol)	Mass (g)
1,4-dibromobutane	0.019	4.097
1-vinylimidazole	0.19	17.4898
2,6-di-tertbutylphenol	0.0013	0.2762

Table 5. Quantities of the chemicals used for the synthesis of 1,1´-butane-1,4-diylbis(3-vinyl imidazolium) dibromide.

2.2.3 Homopolymer sythesis

Poly(4-vinylbenzyl chloride) is synthesized via RAFT polymerization. All the reagents in a flask (Tab. 6) are isolated from oxygen under nitrogen flux for 45 minutes. The reaction is carried out at 100°C for 24 hours. The product is diluted with MeOH and distilled water then dialysed against water for one week, changing the water twice per day. The structure is ascertained by NMR in MeOD.

Chemical	Quantity	Molar ratio
[(4-vinylbenzyl)trialkyl]ammonium	4.4822 g	200
2,2'-azobis(2-methylpropionitrile)	1.8 mg	1
2-cyano-2-propylbenzodothionate	18.6 mg	10
DMF	6.7 mL	

Table 6. Quantities of the chemicals for the homopolymer synthesis.

2.3 Instrumentation and sample preparation

2.3.1 Nuclear Magnetic Resonance

The NMR measurements are performed on a Bruker Avance III 500 MHz spectrometer. The sample are prepared using few mg of polymer and MeOD as a solvent. ^{1}H NMR spectra were measured.

2.3.2 Dynamic Light Scattering

The sample are prepared in the apposite cuvette after cleaning them with distilled water and methanol. The cuvette with the sample is degassed before permforming the measurement. Measurements are carried out at 20°C with a Brookhaven Instruments BI-200SM goniometer, a BI-9000AT digital correlator and a Coherent Sapphire laser 488-100 CDRH operating at the wavelength of 488 nm, 50 mW of power, a pinhole of 200 μm, moving the goniometer from 50° to 140° every 10°. The samples are made of the microgels alone as well as adding NaCl at different concentrations. The samples made of the microgels loaded with the nanoparticles diluted with distilled water at a concentration of 0.5 mg/mL are also measures with DLS. Particle size measurements were performed on Malvern Instruments ZetaSizer Nano-ZS equipped with a 4 mW HeNe laser operating at wavelength 633 nm. A temperature programme is made from 10°C to 90°C at intervals of 2°C. The sample is made of the microgel in water in a known concentration. The cuvettes are cleaned with distilled water and methanol and the samples are degassed.

2.3.3 Fluorescence spectroscopy

The transmittance measurements were performed on a Jasco V-750 spectrophotometer. Samples are prepared always with the same concentration of microgel in water and a fixed amount of pyrene-water previously made as well as with ANS (8-Anilinonaphthalene-1-sulfonic acid). Cuvettes used are cleaned with distilled water and methanol and the sample is degassed before the measurement. The emission spectra is recorded in the range of temperature from 10°C to 90°C.

2.3.4 UV spectroscopy

Jasco V-750 spectrophotometer with temperature control system is used. Samples are made with microgel and water in a fixed concentration. Cuvettes are cleaned with distilled water and methanol and the samples are degassed prior starting the measurements. The temperature programme used goes from 5°C to 90°C. Prior the analysis the sample is stabilized for 10 minutes at the starting temperature, during the measurements the temperature rate is 1°C/min.

2.4 Catalytic application

The as mentioned synthesized microgels are loaded with AuNP to carry out a catalysis experiment to verify a possible application.

2.4.1 Preparation of the microgel-supported AuNP

10 mg of microgel are stirred for one hour with 10 mL of distilled water. $HAuCl_4$ is added to the solution in different proportions of 50%, 100% and 150% per repeting unit (Tab. 7), previously dissolved in a small amount of water, and the solution is stirred for half an hour.

The solution is then dialysed for one day against water in order to remove the excess of $AuCl^-$. After that, $NaBH_4$ is added to the solution dropwise and the reaction is carried out for one hour under stirring. The obtained microgel loaded with AuNP is stored at ambient temperature the half of it and freeze dried and stored in the freezer the other half.

Proportion	Quantity (g)
50	0.0076
100	0.0153
150	0.0229

Table 7. Quantities of $HAuCl_4$ for the gold nanoparticles synthesis.

2.4.2 Thermogravimetric analysis

TGA is performed using the freeze dryed sample around 0.3 mg for the microgel alone as well as the microgel-supported AuNPs. The sample is placed on an aluminium oxide cup apposite for TGA analysis, previously cleaned for one day in acqua regia (nitric acid and hydrocloric acid with a volume ratio of 1:3) and dryed in an oven at 1200°C. The analysis is carried out in a temperature range between 25°C and 800°C. The difference between the two analysis shows the content of gold nanoparticles present on the sample.

2.4.3 Catalysis experiment

The reduction of 4-nitrophenol is carried out directly in a quartz cuvette suitable for the UV-vis spectrometer.

1 mL of $NaBH_4$ (3 mg/mL) is placed in the cuvette together with 1 mL of 4-nitrophenol (0.012 M) and the solution is bubbled with N_2 for 30 minutes. The microgel loaded with AuNP is diluted with water to gain a concentration of 1.5 mg/mL, then diluted again with water 10 times the volume and finally 0.5 mL are taken and mixed with 0.5 mL of water and bubbled with N_2 for 30 minutes. The microgel is added to the solution containing the reagents and it is immediately placed in the UV-vis spectrometer in order to record the spectra of the reduction over time.

3 Results and discussion

3.1 Polymerization process

The monomer is synthesized following the reaction in figure 10.

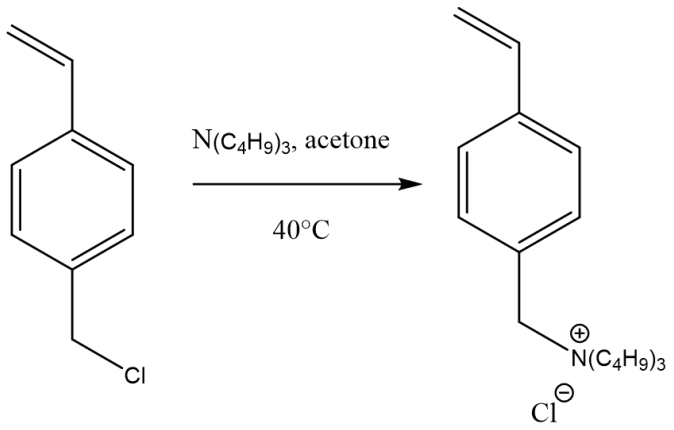

Figure 10. Monomer synthesis reaction.

The calculated yields of this synthesis is 61%, corresponding to 13.561 g.

The synthesis reaction of the microgels is presented in figure 11.

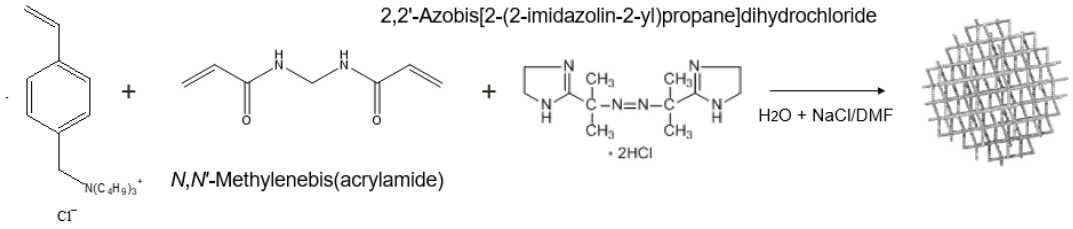

Figure 11. Microgels synthesis reaction.

In table 8 are reported the yields of the microgels synthesized in different conditions.

Microgel	Yield (%)	Yield (g)	Concentration (w/w)
NaCl 0.75 M	59	29.4596	0.001937
NaCl 1 M	/	/	/
NaCl 1.5 M	/	/	/
DMF 30%	42	20.7569	0.003515
DMF 50%	57	28.3008	0.002286
DMF 70%	57	28.7006	0.001180
DMF 90%	36	17.9530	0.000584
$NaNO_3$	48	24.1643	0.002124

Table 8. Microgels yields in 50 mL solution.

The microgels syntheses with 2% of crosslinker and with a different crosslinker were analysed by NMR and the results did not show the peaks corresponding to the monomer, indeed it is not possible to confirm the product.

The real concentration of the microgels in the corresponding solutions are calculated from the dried weight of a certain amount of polymer solution and are reported in table 8.

The NMR spectra to confirm the structures are in Appendix. In the monomer spectra each peak is assigned to an hydrogen of the molecule, the microgels spectra ascertain the syntheses because they present the same peaks of the monomer except the two peaks corresponding to the double bond (g and h). Indeed, during the polymerization the double bond is broken.

The so-mentioned synthesized microgels are tested and studied to investigate the thermoresponsivity and the solution properties.

3.2 Dynamic Light Scattering

DLS measures the hydrodynamic radius R_h, which is, by definition, the radius of a hypothetical hard sphere that diffuses with the same speed as the particle under examination. Polymers in solution are non-spherical, dynamic and solvated, as a consequence the radius calculated from the diffusional properties of the particle indicates the size of the solvated particle. The data obtained are presented as particle size distribution, ob-

tained directly from the instrument, which converts the relaxation time distribution as it is measured, to a particle size distribution, using Stokes-Einstein equation. Since the size of the microgels is unknown, they are not filtered.

DLS analysis at 90° angle, of the microgel synthesized in NaCl solution 0.75 M, with the addition of solutions made of NaCl in water changing the NaCl concentration is shown in figure 12.

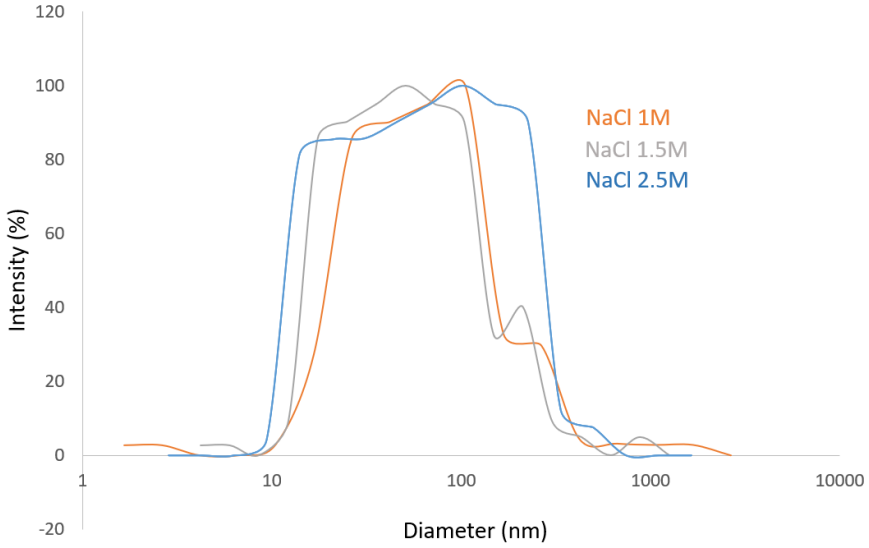

Figure 12. DLS results for the microgel synthesized in NaCl solution 1M measured at 90°.

The average diameter is calculated for the three different NaCl concentration solutions as the arithmetic average media of the diameters of the particles at every angle from 50° to 140° (Tab. 9).

NaCl (M)	**Diameter (nm)**
1	148.66
1.5	106.28
2.5	137.04

Table 9. Average diameter of the microgel synthesized in NaCl solution 1M.

The size distributions are all broad as expected for a polymer in solution since it is a polydisperse sample. However, the average diameter is around the same value in the

three different cases of NaCl addition, which means that the solution properties, are not changed at ambient temperature by addition of salt. In figures 13 and 14 are made comparisons between the dimensions of the particles synthesized in different DMF percentage analysed at 90° angle. In the same way, the average diameter is calculated, the trend is shown in figure 15.

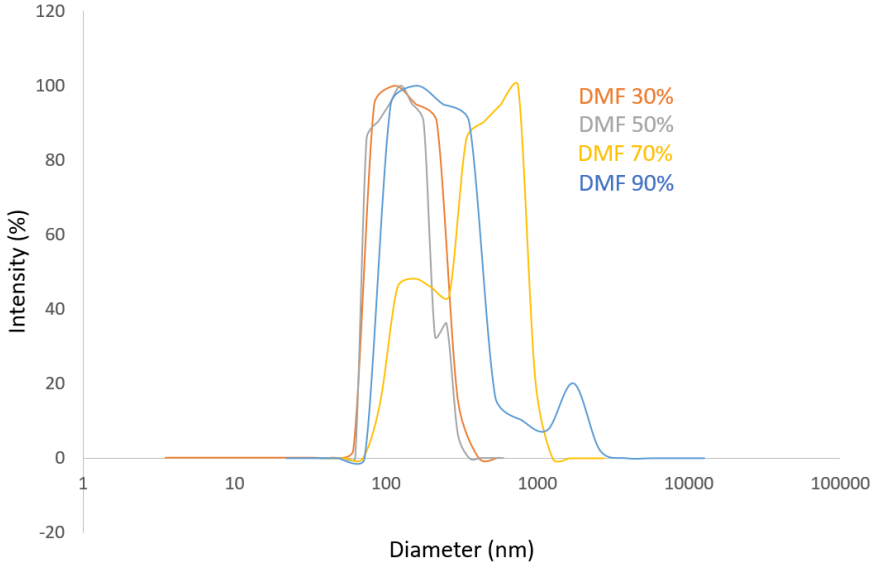

Figure 13. DLS results for the microgels synthesized in DMF solutions measured at 90° without solvent addition.

With the exception of the DMF 90% solution it is noticeable an increase in diameter as the DMF percentage increases. This means that the microgel is more soluble in DMF than water. Indeed the higher percentage of DMF can cause the formation of aggregates as it is possible to see also from the graph. The shoulder present in the size distribution curve of the microgel synthesized in DMF 90% may be caused by some aggregates or dust. The microgel that shows better properties, in terms of diameter and also the most reliable results, resulted to be the one synthesized in DMF 50%. A closer study of this microgel has revealed that at different NaCl solution concentrations added to it, the average diameter does not change, as in the case of the microgel synthesized in NaCl (Fig. 16, Tab. 10). In this case the distribution is wider, so the microgel size is more uniform than in the case of NaCl solution for the synthesis.

The microgels synthesized in DMF 70% and DMF 90% are also studied with DLS after being freeze dried and dissolved (Fig. 17, 18).

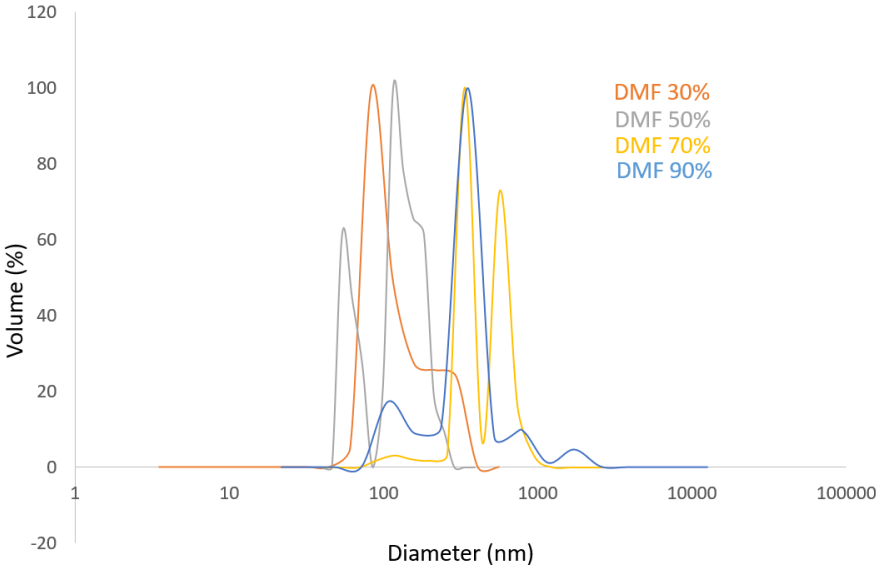

Figure 14. DLS results for the microgel synthesized in DMF solution shown as volume vs. diameter measured at 90°.

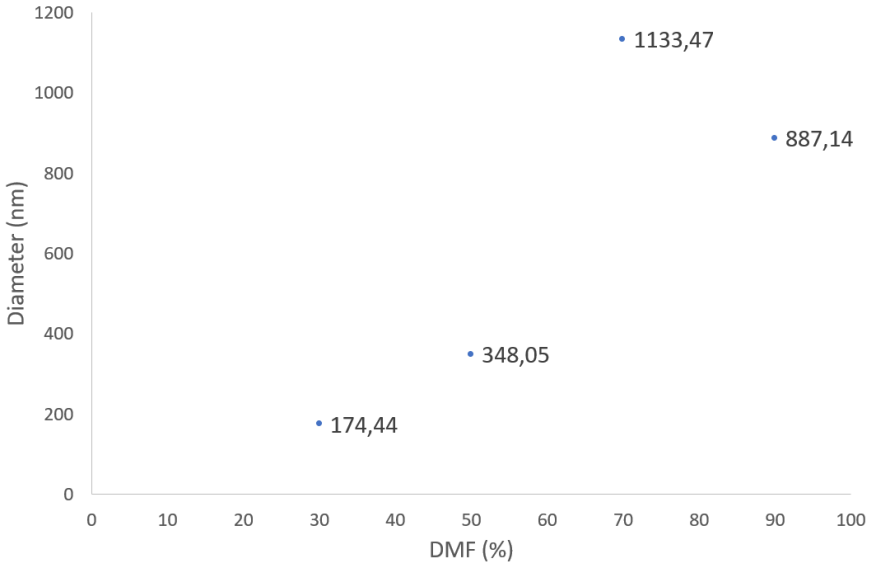

Figure 15. Average diameter of the particles synthesized in DMF solutions without any solvent addition.

The diameter (Tab. 11) in both cases is smaller when the microgel is dissolved. The microgels shrink in presence of water and the measured hydrodynamic radius results to be smaller.

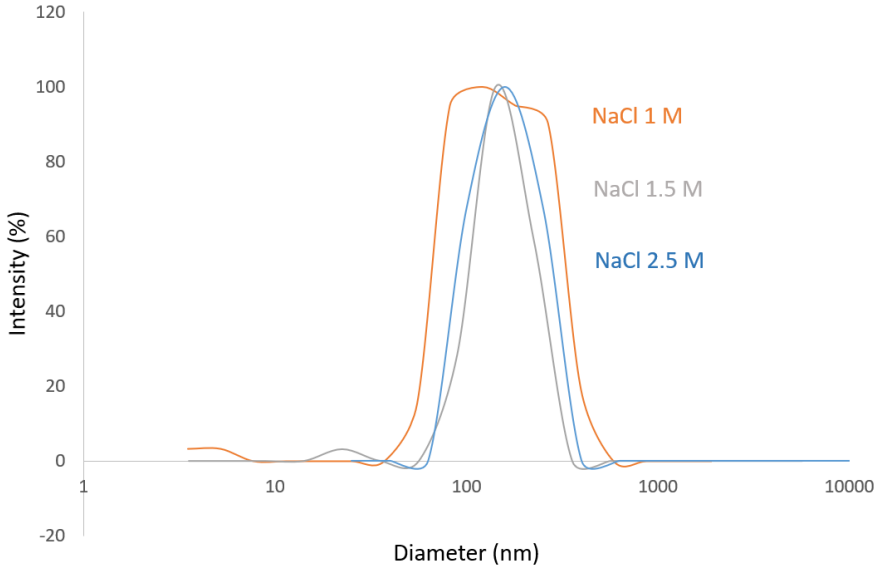

Figure 16. DLS results for the microgel synthesized in DMF 50% solution measured at 90°.

NaCl (M)	Diameter (nm)
1	165.0
1.5	158.1
2.5	169.3

Table 10. Average diameter of the particles in DMF 50% solution.

DMF (%)	Diameter (nm)
70	426.2
70 dissolved	201.9
90	335.0
90 dissolved	256.3

Table 11. Average diameter of the particles in DMF 70% and 90% solutions.

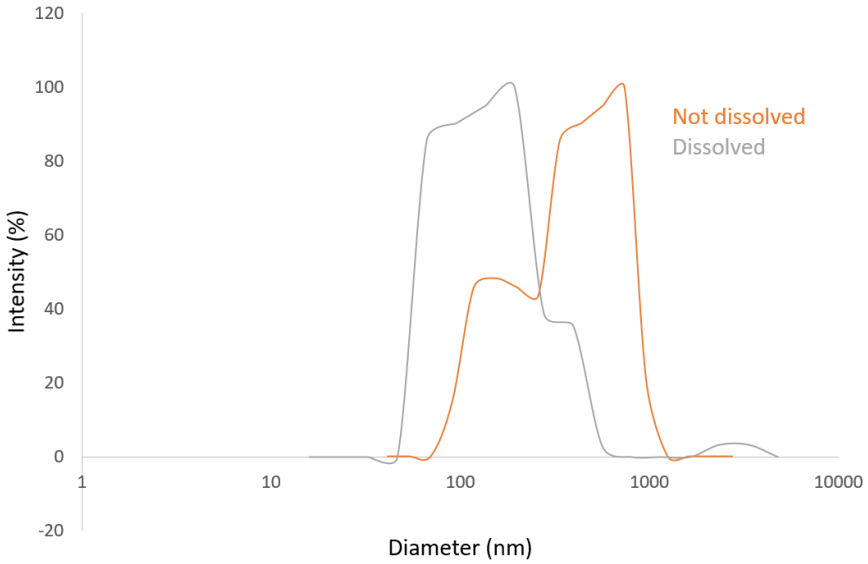

Figure 17. DLS results for the microgel synthesized in DMF 70% solution measured at 90°.

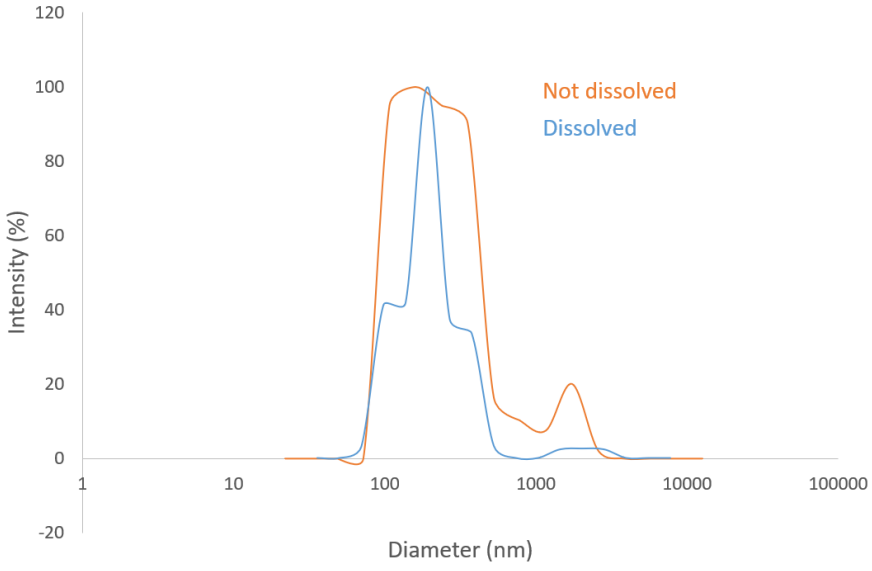

Figure 18. DLS results for the microgel synthesized in DMF 90% solution measured at 90°.

The microgel synthesized in $NaNO_3$ has been analyzed in two different salt concentrations and it shows the same behaviour as the other salts in different concentrations, the average diameter is stable around the same value (Fig. 19, Tab. 12).

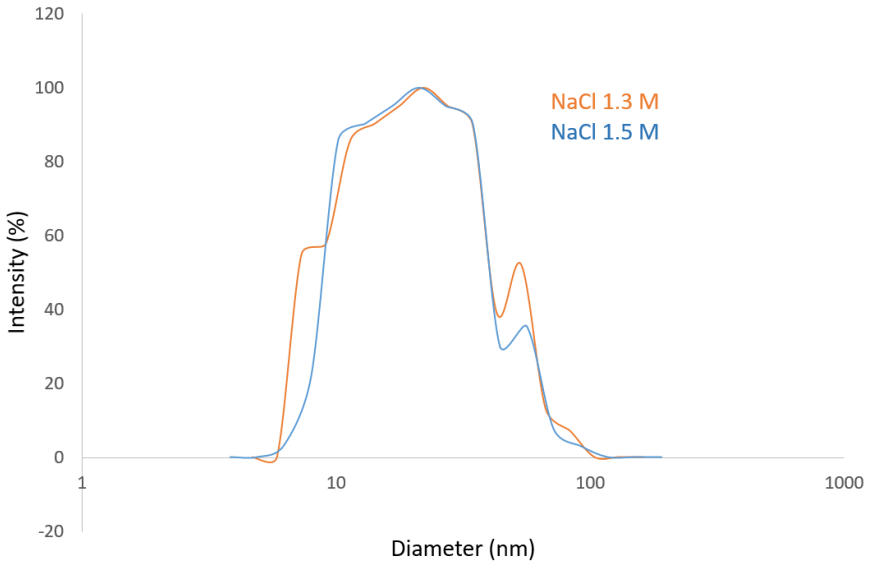

Figure 19. DLS results for the microgel synthesized in $NaNO_3$ solution measured at 90°.

NaCl (M)	**Diameter (nm)**
1.3	37.24
1.5	37.08

Table 12. Average diameter of the particles in $NaNO_3$ solution.

The main difference is in the size which is much smaller compared to other cases. This may be caused by the ionic strenght of the salt which costrains the polyelectrolyte to shrink as a consequence the dimension detected is smaller.
DLS analysis has been performed also to the homopolymer diluted with NaCl acqueous solution 1M. The results are shown in figure 20, it is possible to see two main different distributions.

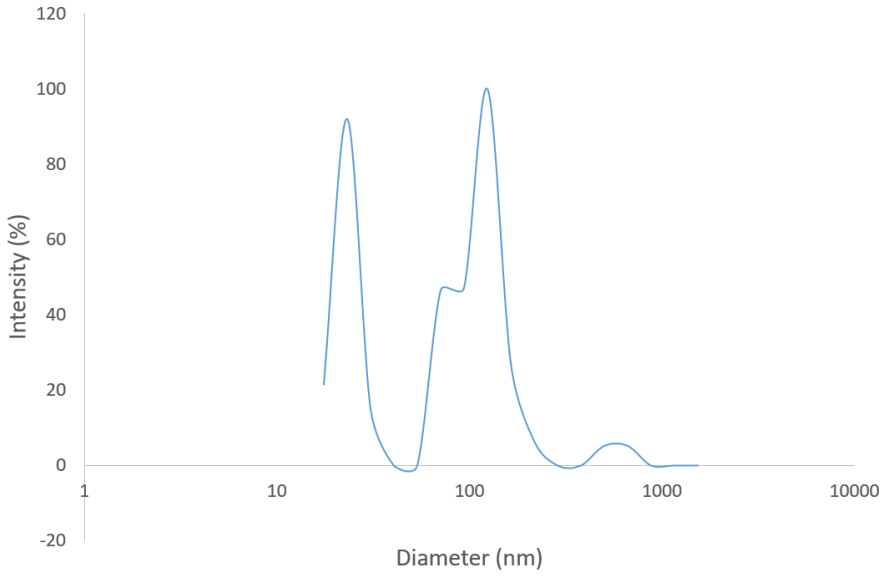

Figure 20. DLS results for the homopolymer with NaCl 1M measured at 90°.

Zetasizer instrument has been used to perfom dynamic light scattering analysis in backscattering mode (173° angle) in a temperature range to follow the size changes of the microgels and test the thermoresponsivity. The results are plotted as temperature vs. diameter, the microgels are analysed with the addition of different NaCl concentrations.
The microgel synthesized in DMF 50% solution results are shown in figures 21 and 22.

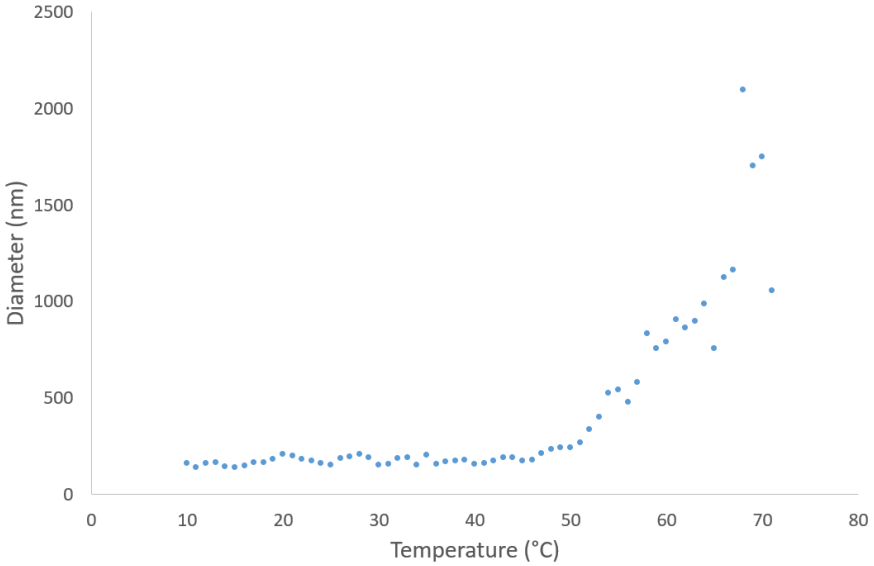

Figure 21. Diameter average of the microgel synthesized in DMF 50% with the addition of NaCl solution 1M as a function of temperature.

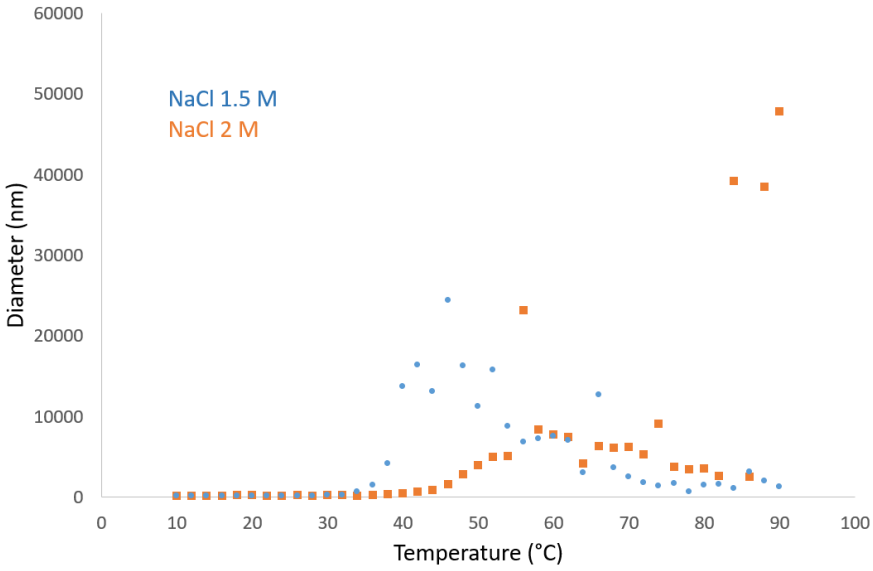

Figure 22. Diameter average of the microgel synthesized in DMF 50% with the addition of NaCl solutions as a function of temperature.

With the addition of 1M NaCl solution the microgel size is very small compared to the other concentrations. We can observe that the microgels size increases with temperature in the case of 1M and 1.5M NaCl solutions. However, when we add 2M NaCl solution we can notice a reversibility that may be caused by the agglomeration of the particles

at high temperature. For the microgel synthesized in DMF 70% solution (Fig. 23) the thermoresponsivity has been tested for the salt concentrations 1.3M and 1.5M. The behaviour shown to be the same as in the DMF 50% solution case, at high temperature the microgel's size tends to increase.

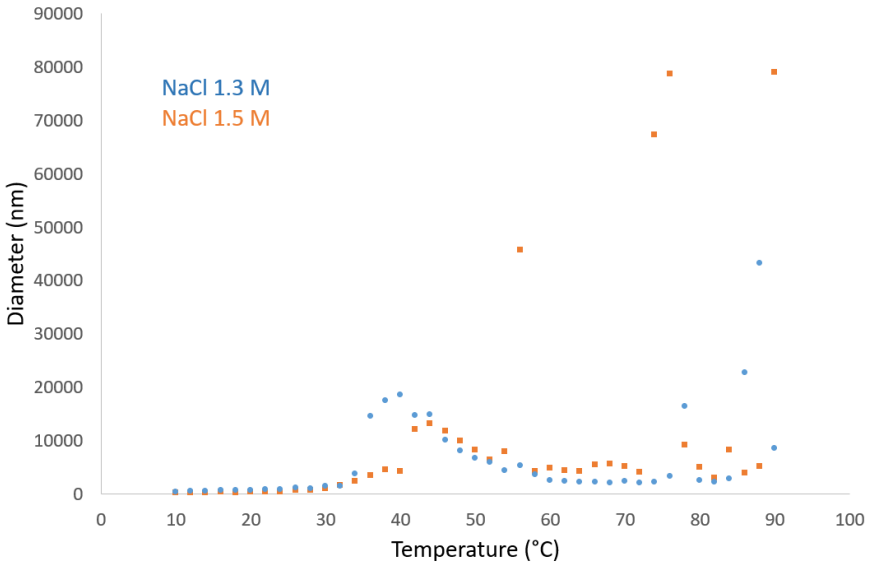

Figure 23. Average diameter of the microgel synthesized in DMF 70% with the addition of NaCl solutions as a function of temperature.

The homopolymer has been also analyzed with the same temperature program by zetasizer instrumentation but it is not possible to follow a trend in this case.

3.3 Fluorescence

Fluorescence measurements are carried out in a wide range of temperature to evidence the cloud point temperature and ascertain the stability of the microgels. Emission spectra are collected using two different probes. Pyrene spectrum (Fig. 24) shows several peaks between 370 and 430 nm. The ratio of the first peak (I_1) to the third (I_3) is reported to correspond to the polarity of the solvent. As a consequence, pyrene has been used referring to this I_1/I_3 method to monitor the hydrophobicity of the microgel in the estabilished range of temperature.[42]

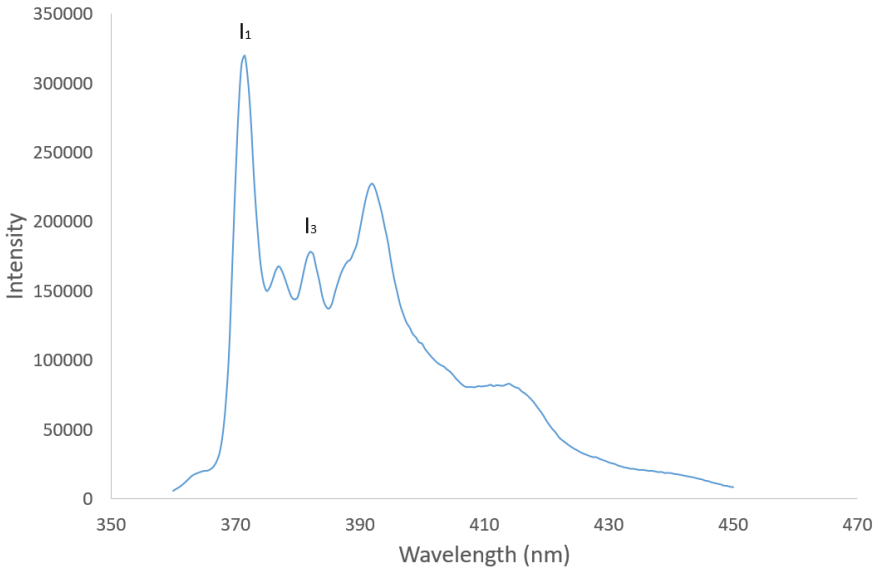

Figure 24. Pyrene emission spectrum.

The microgel synthesized in DMF 50% solution revealed to have the expected behaviour, hence the I_1/I_3 ratio is higher at low temperature and starts to decrease increasing the temperature which means that the hydrophobicity is increasing and the microgel is shrinking. The data are collected in three different environment, three different concentration of NaCl are added to the solution. In all the cases the microgel thermoresponsivity is the same (Fig. 25).

However, from this analysis it is not possible to see a clear transition at the cloud point temperature. Indeed, another fluorescence measurement is carried out with a different probe, ANS, to understand if the problem is the probe. The analysis with ANS shows anyway the same trend but no clear evidence of the cloud point temperature. The microgel synthesized in DMF 70% solution has been also analysed by fluorescence and the results evidence the same thermoresponsive behaviour as the microgel in DMF 50% solution (Fig. 26)

In the case of the homopolymer the trend is different (Fig. 27). It is possible to observe a kind of reversibility from a certain temperature.

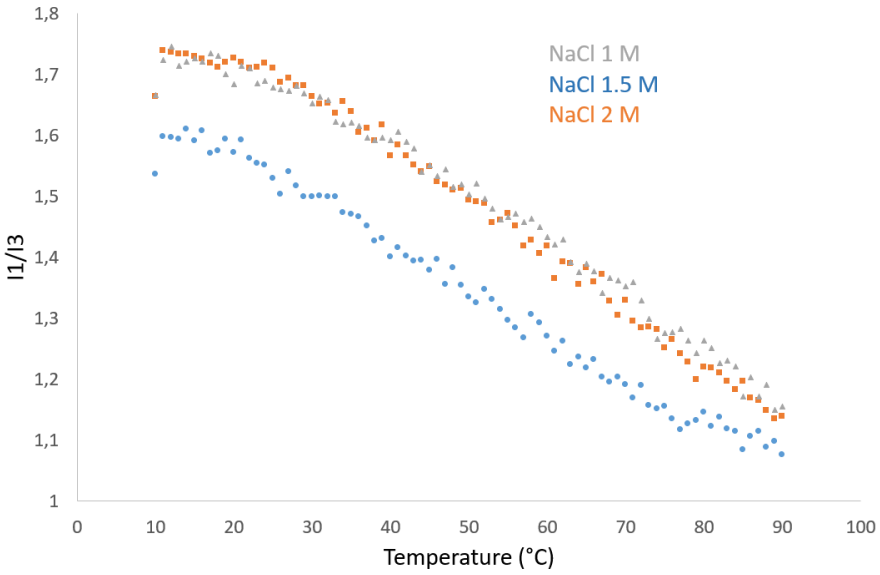

Figure 25. Fluorescence measurement of the microgel sythesized in DMF 50% solution with addition of NaCl acqueous solutions.

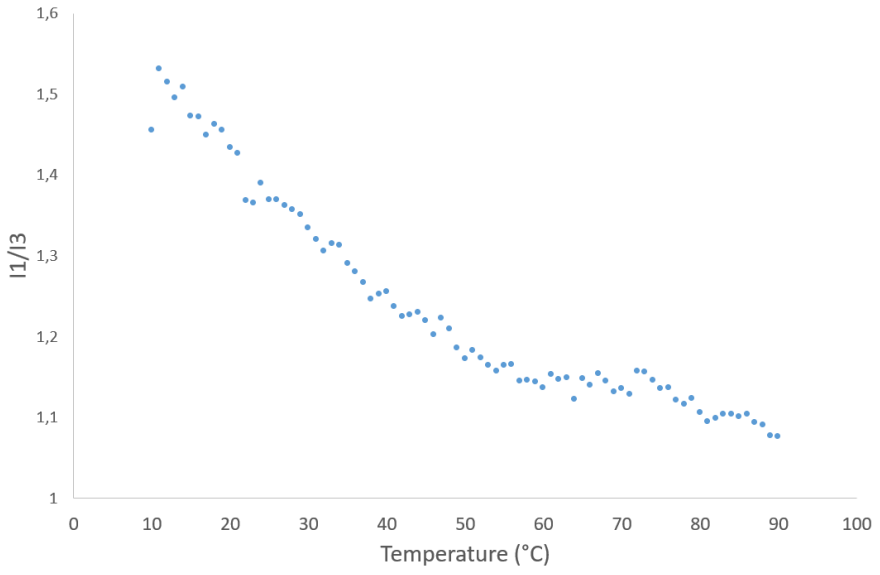

Figure 26. Fluorescence measurement of the microgel sythetized in DMF 70% solution without salt.

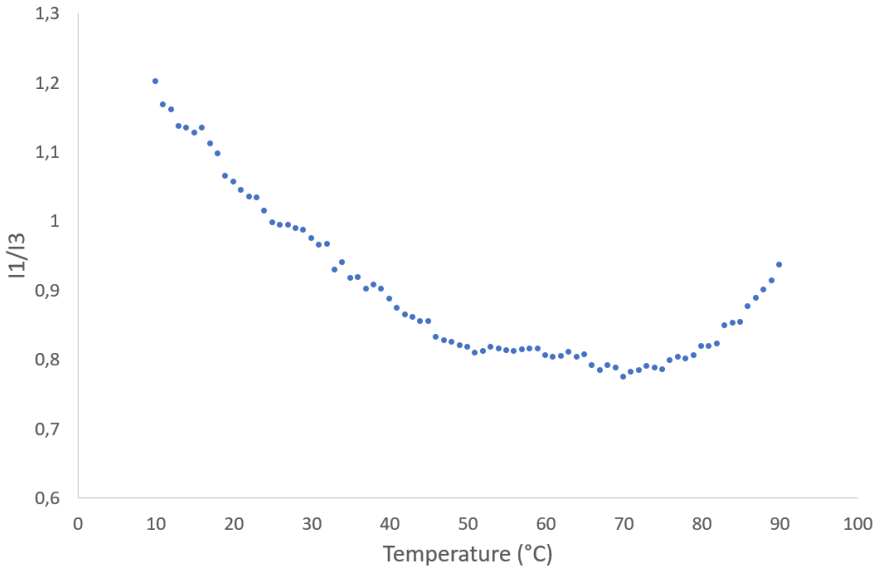

Figure 27. Fluorescence measurement of the homopolymer with the addition of a acqueous solution of NaCl 1.5 M.

3.4 UV-spectroscopy

From the UV analysis the cloud point temperature (T_c) can been clearly seen and calculated. The graphs show an LCST type phase transition, and they reflect the cloud point temperature on the concentration of NaCl. From the spectra it is possible to see a net change in absorbance intensity from one form to another of the microgel. The first step of the phase separation is the breaking up of the ordered water structure around the polymer coil, followed by the collapse of the polymer molecule into a hydrophilic globule. Polymer-polymer interactions are responsible for the aggregation and the subsequent precipitation of the polymer solution.[11]

A different concentrated NaCl solution is added to every microgel in order to observe any change or shift in the T_c. From this analysis the T_c can be calcuted as the maximum of the differential of transmittance respect to the temperature at a certain wavelength. The microgel synthesized in DMF 30% solution results are reported in figure 28 where it is possible to observe a deacrease in T_c increasing the NaCl concentration. The calculated T_c values are reported in figure 29.

The same analysis has been carried out for the microgels synthesized in the solutions DMF 50% and DMF 70% (Fig. 30, 31).

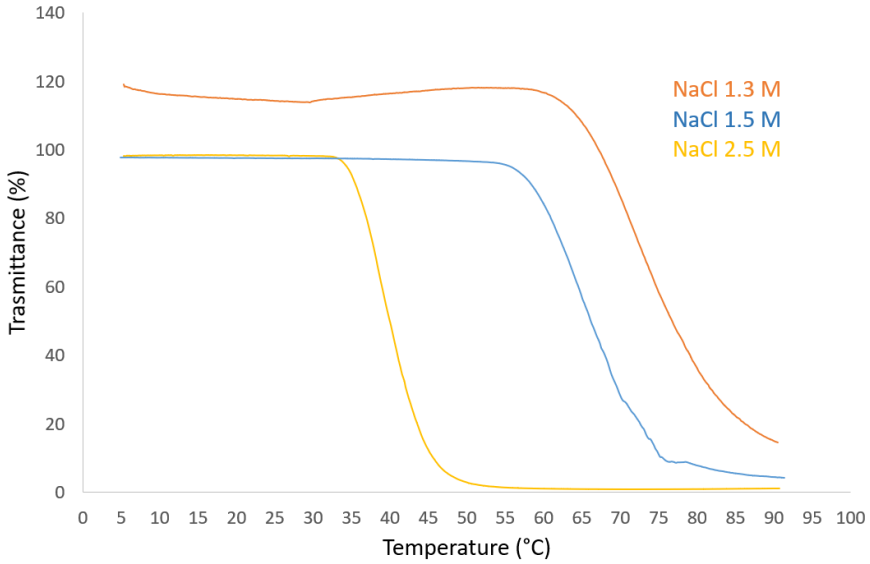

Figure 28. UV measurements of the microgel synthesized in DMF 30% solution with different NaCl concentration added.

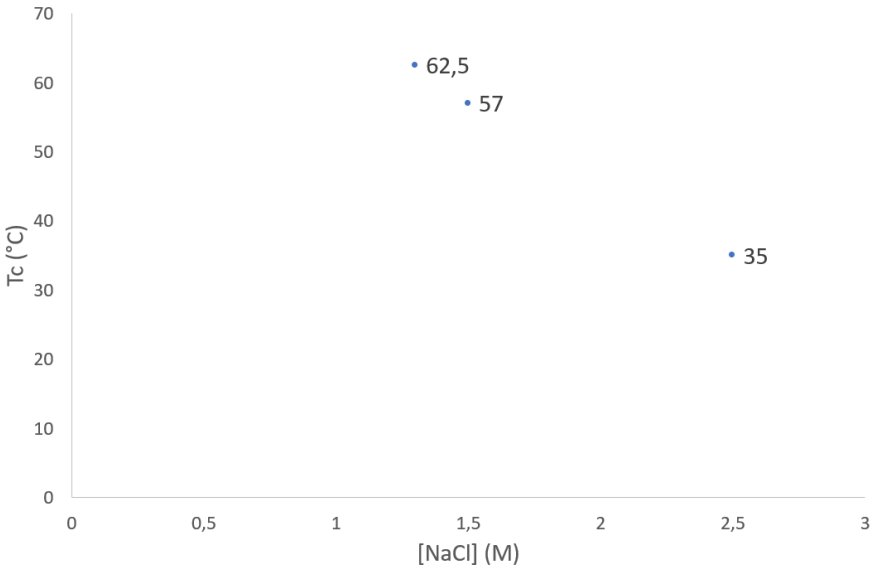

Figure 29. Cloud point temperature of the microgel synthesized in DMF 30% solution.

In figures 32 and 33 are reported the cloud point temperatures.

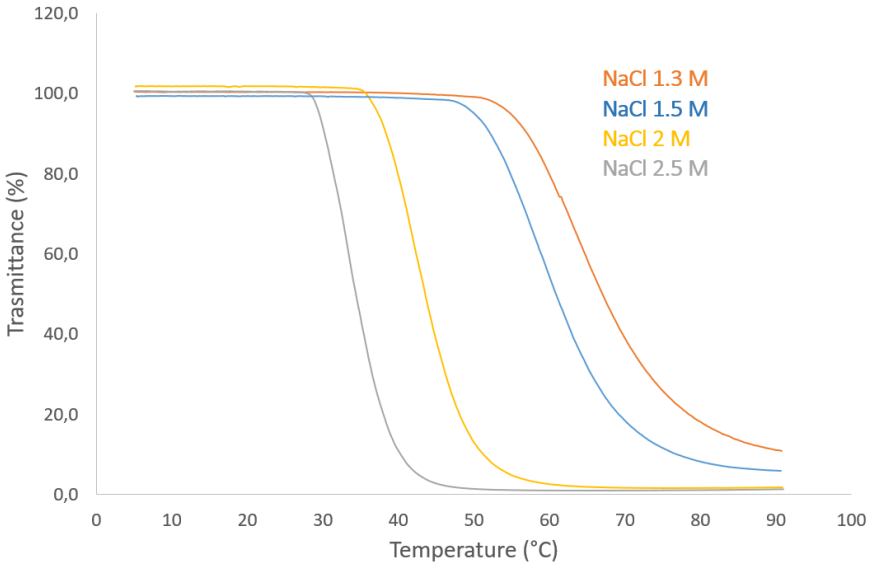

Figure 30. UV measurements of the microgel synthesized in DMF 50% solution with different NaCl concentration added.

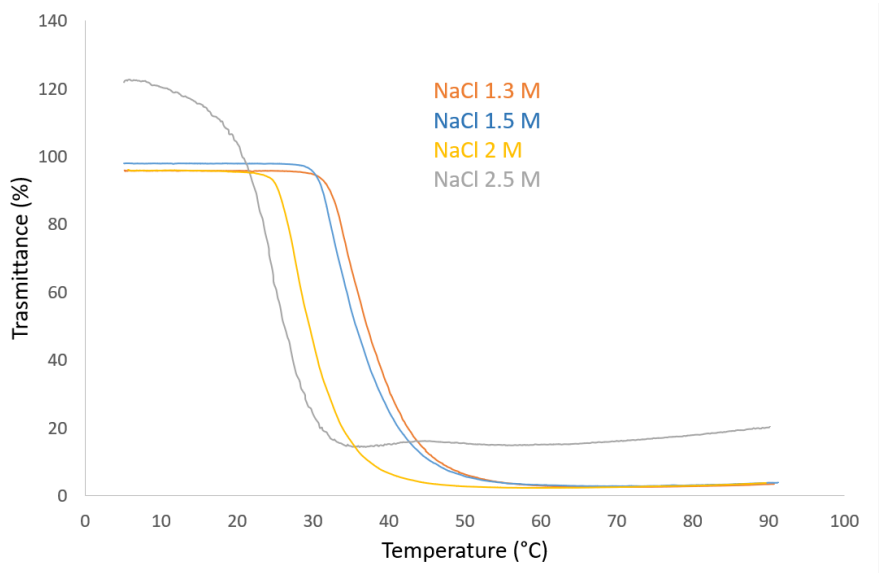

Figure 31. UV measurements of the microgel synthesized in DMF 70% solution with different NaCl concentration added.

Comparing all the results obtained it is possible to notice that in all the cases the T_c decreases increasing the NaCl concentration. The coil structure of the microgel at high salt concentration is more shrinked due to polyelectrolyte effect, as a consequence, it changes into a globule-like conformation at lower temperature, as hydration levels decrease and hydrophobic interactions increase.

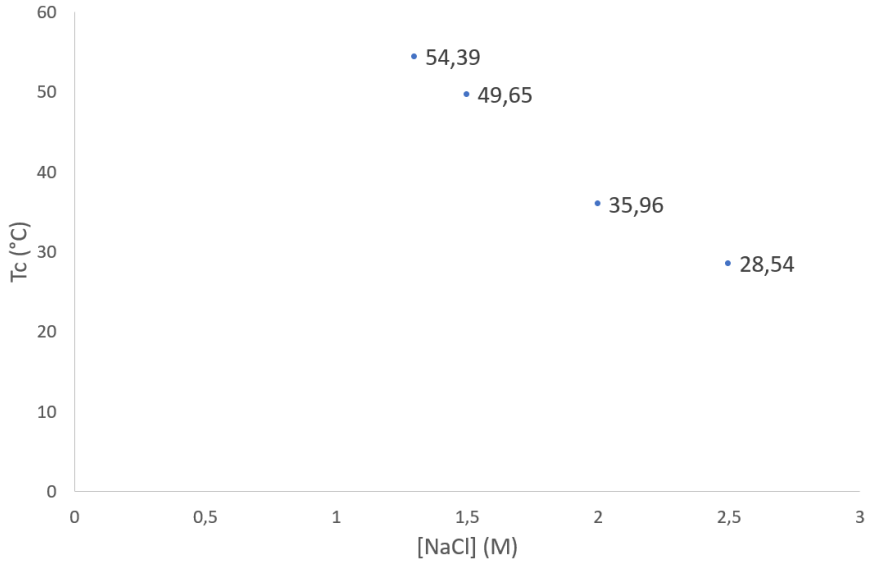

Figure 32. Cloud point temperature of the microgel synthesized in DMF 50% solution.

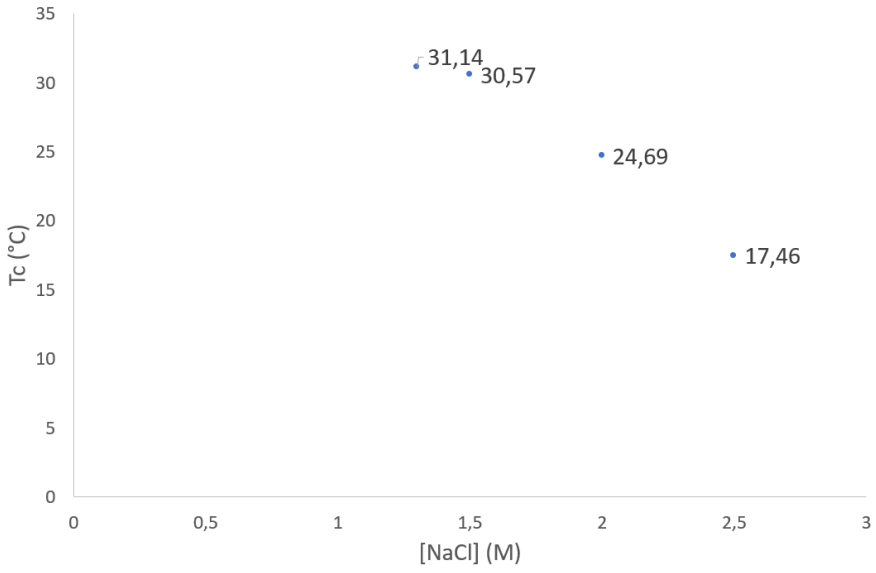

Figure 33. Cloud point temperature of the microgel synthesized in DMF 70% solution.

The addition of NaCl increases the ionic strength of the system, allowing the polymer

to show LCST type phase transition. Cl^- ions compete to bind the positively charged polymer chain. At low temperature the Cl^- clouds formed around the chain shield the polymer so the transmittance is higher. At high temperature the polymer dissociate more and the transmittance results to be lower.

Moreover, having a closer look we can see that for the same concentration, different microgels have different T_c. In particular, the T_c decreases increasing the DMF percentage in the synthesis solution. The same analysis carried out for the homopolymer has given the same trend as a result (Fig. 34, 35).

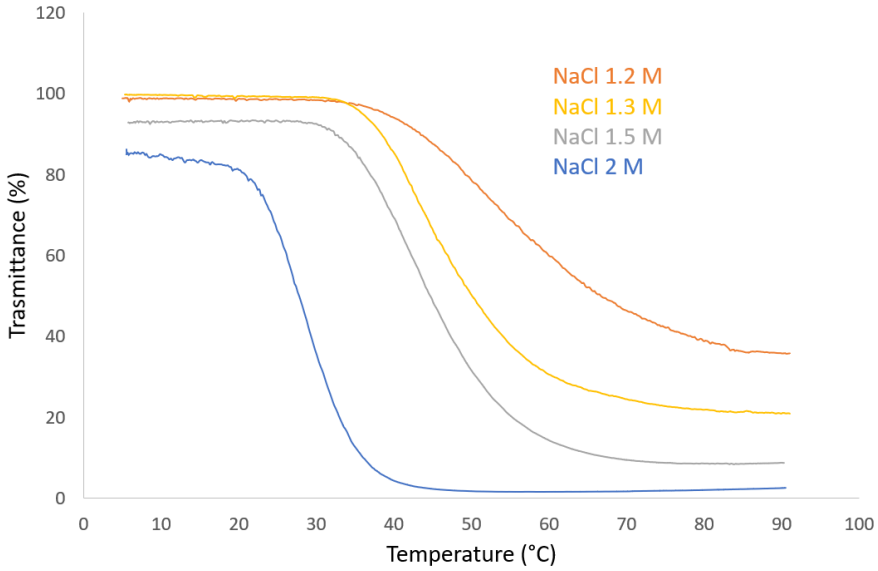

Figure 34. UV measurements of the homopolymer.

The range of temperature is also close to the microgels ranges.

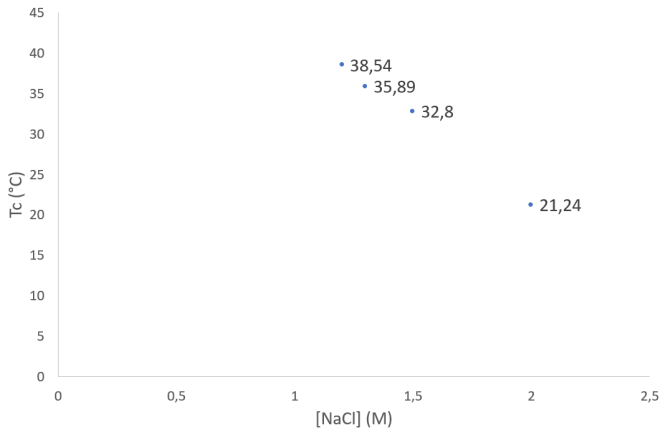

Figure 35. Cloud point temperature of the homopolymer.

3.5 Microgel-supported AuNP

The generation of AuNPs takes place within the most external layer. The successful exchange of the counter ions in the brush layer is highlighted by a yellowish colour (Fig. 36). While the reduction of $AuCl^-$ is clearly seen by the change in colour from yellow to violet (Fig. 37).

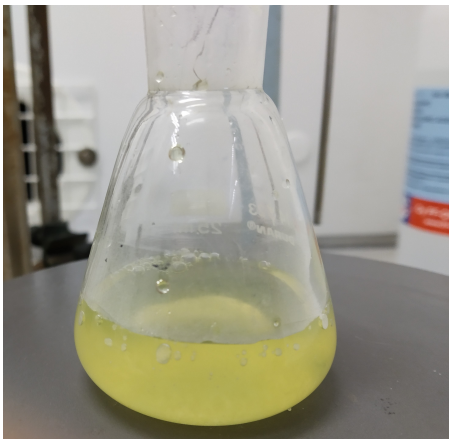

Figure 36. Microgel-supported AuNPs before reduction.

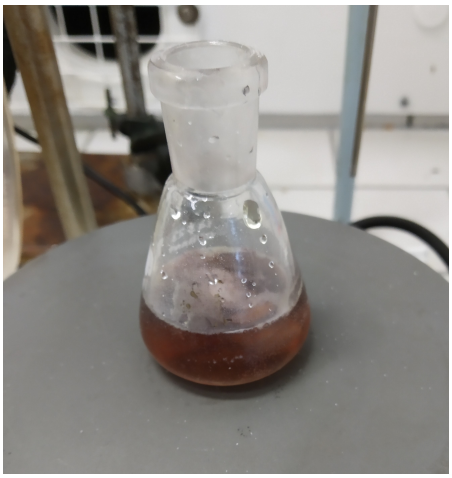

Figure 37. Microgel-supported AuNPs after reduction.

The thickness of the brush layer, L, can be calculated from the hydrodynamic radius of the particles measured by DLS. Since the radius of the core particle, R, is calculated from DLS (calculated in section 3.2 Fig. 13), the thickness of the surface layer can be calcuated as L = R - R_h, where R_h is the measured hydrodynamic radius for the AuNPs supported onto the microgel which is 161 nm (Fig. 38). The decrease of the surface

layer thickness results to be 12 nm.

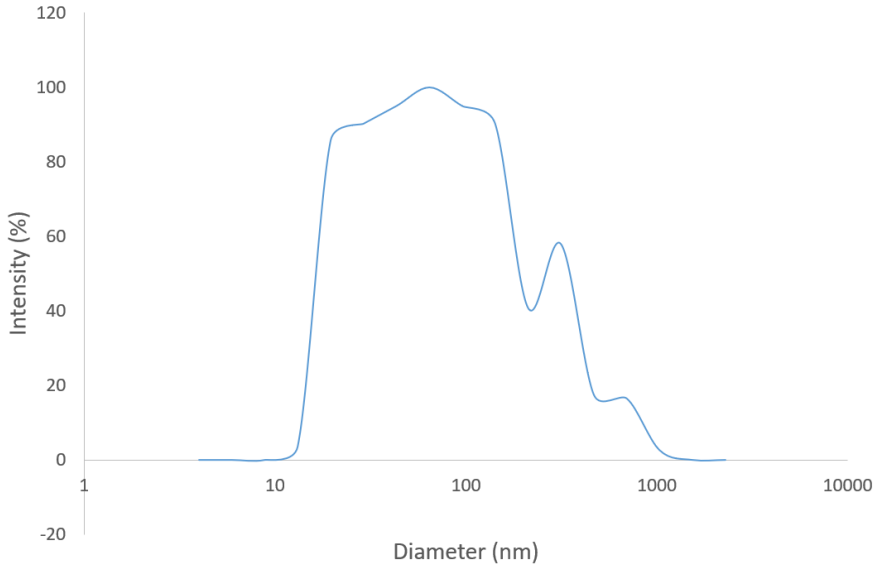

Figure 38. DLS result for the AuNPs decorated microgel synthesisez in DMF 30% measured at 90°.

The amount of AuNPs loaded in the microgel has been calculated by TGA analysis (Fig. 39). The microgel degradation has two main steps. The degradation of the microgel decorated with AuNPs shows the same steps of the microgel without AuNPs. This fact can prove that the microgel is not modified by the formation of AuNPs on it. Moreover, the difference between the remaining material when the microgel is loaded with AuNPs and when is not reveals the amount of AuNPs present, which is shown to be 32%.
The catalytic experiment has been run but it did not show a successful result.

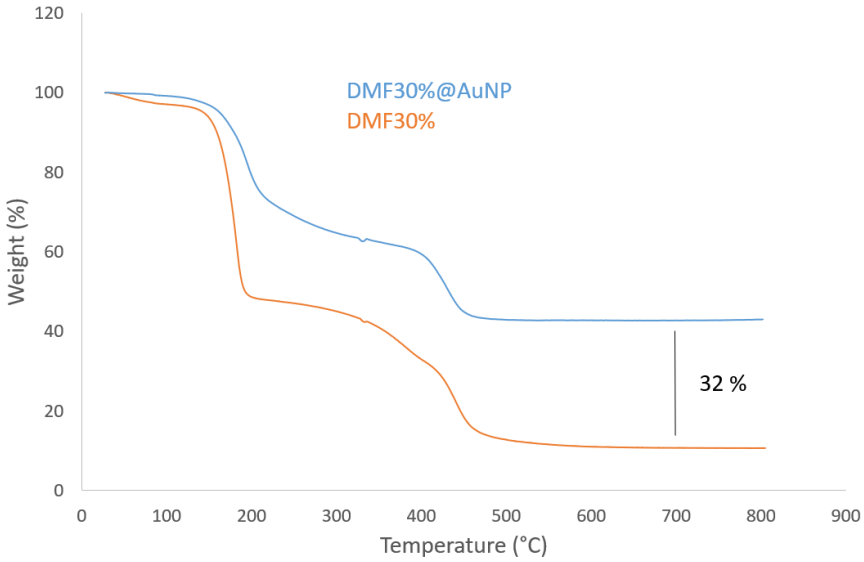

Figure 39. Thermogravimetric analysis of the microgel synthesized in DMF 30% with and without the AuNPs.

4 Conclusions

The novel series of thermoresponsive microgels synthesized shown to be successful in terms of synthesis as well as in terms of thermoresponsivity.

The size is measured to be in the range between 100 nm and 200 nm from the DLS anaysis and the structure is confirmed by ^{1}H NMR. Fluorescence analysis in a temperature program method as well as turbidimetry and DLS with zetasizer, show the effective thermoresposive behaviour of the microgels. Indeed, they shrink with high temperature, they undergo a coil-to-globule transition which has been proved to be tunable by addition of certain concentrations of salt. It is safe to assume that these microgels are stable in the temperature range between 5°C and 80°C.

One of the possible applications of these microgels is as stabilizers for nanoparticles for catalytic purposes. The loading of the nanoparticels as well as the catalysis experiment itself have been carried out in a successful way. AuNPs are implemented in the microgels and TGA and DLS analysis confirmed that the nanoparticles are present and they have the proper range of size compared to literature. The TGA analysis shows that 32% of the microgle-supported AuNPs is effectively AuNPs while DLS shows that the brush layer is reduced by the addition of AuNPs.

Future research can be focused on more experiments to estabilish a dependence to different salt (more than NaCl tested in this work), as well as different catalysis experiments to proof their utility in this field.

References

[1] Menglian Wei, Yongfeng Gao, Xue Li, and Michael J Serpe. Stimuli-responsive polymers and their applications. *Polymer Chemistry*, 8(1):127–143, 2017.

[2] Qilu Zhang, Christine Weber, Ulrich S Schubert, and Richard Hoogenboom. Thermoresponsive polymers with lower critical solution temperature: from fundamental aspects and measuring techniques to recommended turbidimetry conditions. *Materials Horizons*, 4(2):109–116, 2017.

[3] Clinton D Jones and L Andrew Lyon. Shell-restricted swelling and core compression in poly (n-isopropylacrylamide) core- shell microgels. *Macromolecules*, 36(6):1988–1993, 2003.

[4] Erno Karjalainen, Vitaliy Khlebnikov, Antti Korpi, Sami-Pekka Hirvonen, Sami Hietala, Vladimir Aseyev, and Heikki Tenhu. Complex interactions in aqueous pil-pnipam-pil triblock copolymer solutions. *Polymer*, 58:180–188, 2015.

[5] Wu Xu, Emanuel I Cooper, and C Austen Angell. Ionic liquids: ion mobilities, glass temperatures, and fragilities. *The Journal of Physical Chemistry B*, 107(25):6170–6178, 2003.

[6] Yongjun Men, Danuta Kuzmicz, and Jiayin Yuan. Poly (ionic liquid) colloidal particles. *Current opinion in colloid & interface science*, 19(2):76–83, 2014.

[7] Yicheng Zhu, Rhiannon Batchelor, Andrew B Lowe, and Peter J Roth. Design of thermoresponsive polymers with aqueous lcst, ucst, or both: Modification of a reactive poly (2-vinyl-4, 4-dimethylazlactone) scaffold. *Macromolecules*, 49(2):672–680, 2016.

[8] Felix A Plamper, Matthias Ballauff, and Axel HE Müller. Tuning the thermoresponsiveness of weak polyelectrolytes by ph and light: lower and upper critical-solution temperature of poly (n, n-dimethylaminoethyl methacrylate). *Journal of the American Chemical Society*, 129(47):14538–14539, 2007.

[9] Jan Seuring and Seema Agarwal. First example of a universal and cost-effective approach: Polymers with tunable upper critical solution temperature in water and electrolyte solution. *Macromolecules*, 45(9):3910–3918, 2012.

[10] Erno Karjalainen, Vladimir Aseyev, and Heikki Tenhu. Counterion-induced ucst for polycations. *Macromolecules*, 47(21):7581–7587, 2014.

[11] I Idziak, D Avoce, D Lessard, D Gravel, and XX Zhu. Thermosensitivity of aqueous solutions of poly (n, n-diethylacrylamide). *Macromolecules*, 32(4):1260–1263, 1999.

[12] Yanjie Zhang, Steven Furyk, David E Bergbreiter, and Paul S Cremer. Specific ion effects on the water solubility of macromolecules: Pnipam and the hofmeister series. *Journal of the American Chemical Society*, 127(41):14505–14510, 2005.

[13] Jan Heyda and Joachim Dzubiella. Thermodynamic description of hofmeister effects on the lcst of thermosensitive polymers. *The Journal of Physical Chemistry B*, 118(37):10979–10988, 2014.

[14] Erno Karjalainen, Vladimir Aseyev, and Heikki Tenhu. Influence of hydrophobic anion on solution properties of pdmaema. *Macromolecules*, 47(6):2103–2111, 2014.

[15] Wolfgang Schärtl. *Light scattering from polymer solutions and nanoparticle dispersions*. Springer Science & Business Media, 2007.

[16] Mark J Stevens and Steven J Plimpton. The effect of added salt on polyelectrolyte structure. *The European Physical Journal B-Condensed Matter and Complex Systems*, 2(3):341–345, 1998.

[17] Hu Yang, Qiang Zheng, and Rongshi Cheng. New insight into "polyelectrolyte effect". *Colloids and Surfaces A: Physicochemical and Engineering Aspects*, 407:1–8, 2012.

[18] S Abrol, MJ Caulfield, GG Qiao, and DH Solomon. Studies on microgels. 5. synthesis of microgels via living free radical polymerisation. *Polymer*, 42(14):5987–5991, 2001.

[19] Andrij Pich and Walter Richtering. *Chemical design of responsive microgels*, volume 234. Springer, 2010.

[20] Susann Schachschal, Andreea Balaceanu, Claudiu Melian, Dan E Demco, Thomas Eckert, Walter Richtering, and Andrij Pich. Polyampholyte microgels with anionic core and cationic shell. *Macromolecules*, 43(9):4331–4339, 2010.

[21] Shoumin Chen, Yahui Peng, Qingshi Wu, Aiping Chang, Anqi Qu, Jing Shen, Jianda Xie, Zahoor H Farooqi, and Weitai Wu. Synthesis and characterization of responsive poly (anionic liquid) microgels. *Polymer Chemistry*, 7(34):5463–5473, 2016.

[22] Brandon V Slaughter, Shahana S Khurshid, Omar Z Fisher, Ali Khademhosseini, and Nicholas A Peppas. Hydrogels in regenerative medicine. *Advanced materials*, 21(32-33):3307–3329, 2009.

[23] Jeong-Yun Sun, Xuanhe Zhao, Widusha RK Illeperuma, Ovijit Chaudhuri, Kyu Hwan Oh, David J Mooney, Joost J Vlassak, and Zhigang Suo. Highly stretchable and tough hydrogels. *Nature*, 489(7414):133, 2012.

[24] Somali Chaterji, Il Keun Kwon, and Kinam Park. Smart polymeric gels: redefining the limits of biomedical devices. *Progress in polymer science*, 32(8-9):1083–1122, 2007.

[25] Artjom Döring, Wolfgang Birnbaum, and Dirk Kuckling. Responsive hydrogels–structurally and dimensionally optimized smart frameworks for applications in catalysis, micro-system technology and material science. *Chemical Society Reviews*, 42(17):7391–7420, 2013.

[26] Jinming Hu, Guoqing Zhang, and Shiyong Liu. Enzyme-responsive polymeric assemblies, nanoparticles and hydrogels. *Chemical Society Reviews*, 41(18):5933–5949, 2012.

[27] Ying Guan and Yongjun Zhang. Boronic acid-containing hydrogels: synthesis and their applications. *Chemical Society Reviews*, 42(20):8106–8121, 2013.

[28] Xiaofan Ji, Bingbing Shi, Hu Wang, Danyu Xia, Kecheng Jie, Zi Liang Wu, and Feihe Huang. Supramolecular construction of multifluorescent gels: Interfacial assembly of discrete fluorescent gels through multiple hydrogen bonding. *Advanced Materials*, 27(48):8062–8066, 2015.

[29] Isidro Cobo, Ming Li, Brent S Sumerlin, and Sébastien Perrier. Smart hybrid materials by conjugation of responsive polymers to biomacromolecules. *Nature materials*, 14(2):143, 2015.

[30] Frederic Hapiot, Stephane Menuel, and Eric Monflier. hydrogels in catalysis. *ACS Catalysis*, 3(5):1006–1010, 2013.

[31] Toyoichi Tanaka and David J Fillmore. Kinetics of swelling of gels. *The Journal of Chemical Physics*, 70(3):1214–1218, 1979.

[32] Chi Wu and Shuiqin Zhou. Volume phase transition of swollen gels: discontinuous or continuous? *Macromolecules*, 30(3):574–576, 1997.

[33] Robert Pelton. Temperature-sensitive aqueous microgels. *Advances in colloid and interface science*, 85(1):1–33, 2000.

[34] Chad E Reese, Alexander V Mikhonin, Marta Kamenjicki, Alexander Tikhonov, and Sanford A Asher. Nanogel nanosecond photonic crystal optical switching. *Journal of the American Chemical Society*, 126(5):1493–1496, 2004.

[35] Beng H Tan and Kam C Tam. Review on the dynamics and micro-structure of ph-responsive nano-colloidal systems. *Advances in Colloid and Interface Science*, 136(1-2):25–44, 2008.

[36] L Andrew Lyon, Zhiyong Meng, Neetu Singh, Courtney D Sorrell, and Ashlee St John. Thermoresponsive microgel-based materials. *Chemical Society Reviews*, 38(4):865–874, 2009.

[37] Johan Mattsson, Hans M Wyss, Alberto Fernandez-Nieves, Kunimasa Miyazaki, Zhibing Hu, David R Reichman, and David A Weitz. Soft colloids make strong glasses. *Nature*, 462(7269):83, 2009.

[38] Rahul Tiwari and Andreas Walther. Strong anionic polyelectrolyte microgels. *Polymer Chemistry*, 6(31):5550–5554, 2015.

[39] Isamu Kaneda, Atsushi Sogabe, and Hideo Nakajima. Water-swellable polyelectrolyte microgels polymerized in an inverse microemulsion using a nonionic surfactant. *Journal of colloid and interface science*, 275(2):450–457, 2004.

[40] H Nur, VT Pinkrah, JC Mitchell, LS Benée, and MJ Snowden. Synthesis and properties of polyelectrolyte microgel particles. *Advances in colloid and interface science*, 158(1-2):15–20, 2010.

[41] Jochen Kleinen and Walter Richtering. Polyelectrolyte microgels based on poly-n-isopropylacrylamide: Influence of charge density on microgel properties, binding of poly-diallyldimethylammonium chloride, and properties of polyelectrolyte complexes. *Colloid and Polymer Science*, 289(5-6):739, 2011.

[42] Jukka Niskanen, Cynthia Wu, Maggie Ostrowski, Gerald G Fuller, Heikki Tenhu, and Sami Hietala. Interfacial and fluorescence studies on stereoblock poly (n-isopropylacryl amide) s. *Langmuir*, 28(41):14792–14798, 2012.

[43] Guillermina Burillo, Emilio Bucio, Ever Arenas, and Gabriel P Lopez. Temperature and ph-sensitive swelling behavior of binary dmaema/4vp grafts on poly (propylene) films. *Macromolecular Materials and Engineering*, 292(2):214–219, 2007.

[44] Erno Karjalainen, Vladimir Aseyev, and Heikki Tenhu. Upper or lower critical solution temperature, or both? studies on cationic copolymers of n-isopropylacrylamide. *Polymer Chemistry*, 6(16):3074–3082, 2015.

[45] Ingo Berndt, Jan Skov Pedersen, and Walter Richtering. Structure of multiresponsive "intelligent" core- shell microgels. *Journal of the American Chemical Society*, 127(26):9372–9373, 2005.

[46] Fumihiko Tanaka, Tsuyoshi Koga, and Francoise M Winnik. Temperature-responsive polymers in mixed solvents: competitive hydrogen bonds cause cononsolvency. *Physical review letters*, 101(2):028302, 2008.

[47] Krzysztof Matyjaszewski and Thomas P Davis. *Handbook of radical polymerization*. John Wiley & Sons, 2003.

[48] Erno Karjalainen, Naveen Chenna, Pasi Laurinmäki, Sarah J Butcher, and Heikki Tenhu. Diblock copolymers consisting of a polymerized ionic liquid and poly (n-isopropylacrylamide). effects of pnipam block length and counter ion on self-assembling and thermal properties. *Polymer Chemistry*, 4(4):1014–1024, 2013.

[49] Christopher Barner-Kowollik. *Handbook of RAFT polymerization*. John Wiley & Sons, 2008.

[50] Jérôme Claverie, Christian Pichot, et al. *Polymers in Dispersed Media II: International Conference on Polymers in Dispersed Media*, volume 2. John Wiley & Sons, 2000.

[51] Howard G Schild. Poly (n-isopropylacrylamide): experiment, theory and application. *Progress in polymer science*, 17(2):163–249, 1992.

[52] Yu Mei, Geeta Sharma, Yan Lu, Matthias Ballauff, Markus Drechsler, Thorsten Irrgang, and Rhett Kempe. High catalytic activity of platinum nanoparticles immobilized on spherical polyelectrolyte brushes. *Langmuir*, 21(26):12229–12234, 2005.

[53] Yu Mei, Yan Lu, Frank Polzer, Matthias Ballauff, and Markus Drechsler. Catalytic activity of palladium nanoparticles encapsulated in spherical polyelectrolyte brushes and core- shell microgels. *Chemistry of Materials*, 19(5):1062–1069, 2007.

[54] Snigdhamayee Praharaj, Sudip Nath, Sujit Kumar Ghosh, Subrata Kundu, and Tarasankar Pal. Immobilization and recovery of au nanoparticles from anion exchange resin: resin-bound nanoparticle matrix as a catalyst for the reduction of 4-nitrophenol. *Langmuir*, 20(23):9889–9892, 2004.

[55] Jiayin Yuan, Stefanie Wunder, Franziska Warmuth, and Yan Lu. Spherical polymer brushes with vinylimidazolium-type poly (ionic liquid) chains as support for metallic nanoparticles. *Polymer*, 53(1):43–49, 2012.

[56] Xian-Jing Zhou, Hai-Peng Lu, Ling-Li Kong, Dong Zhang, Wei Zhang, Jing-Jing Nie, Jia-Yin Yuan, Bin-Yang Du, and Xin-Ping Wang. Thermo-sensitive microgels supported gold nanoparticles as temperature-mediated catalyst. *Chinese Journal of Polymer Science*, 37(3):235–242, 2019.

[57] Marie-Christine Daniel and Didier Astruc. Gold nanoparticles: assembly, supramolecular chemistry, quantum-size-related properties, and applications toward biology, catalysis, and nanotechnology. *Chemical reviews*, 104(1):293–346, 2004.

[58] Sudipa Panigrahi, Soumen Basu, Snigdhamayee Praharaj, Surojit Pande, Subhra Jana, Anjali Pal, Sujit Kumar Ghosh, and Tarasankar Pal. Synthesis and size-selective catalysis by supported gold nanoparticles: study on heterogeneous and homogeneous catalytic process. *The Journal of Physical Chemistry C*, 111(12):4596–4605, 2007.

[59] Marc Schrinner, Frank Polzer, Yu Mei, Yan Lu, Björn Haupt, Matthias Ballauff, Astrid Göldel, Markus Drechsler, Johannes Preussner, and Uwe Glatzel. Mechanism of the formation of amorphous gold nanoparticles within spherical polyelectrolyte brushes. *Macromolecular Chemistry and Physics*, 208(14):1542–1547, 2007.

Appendix

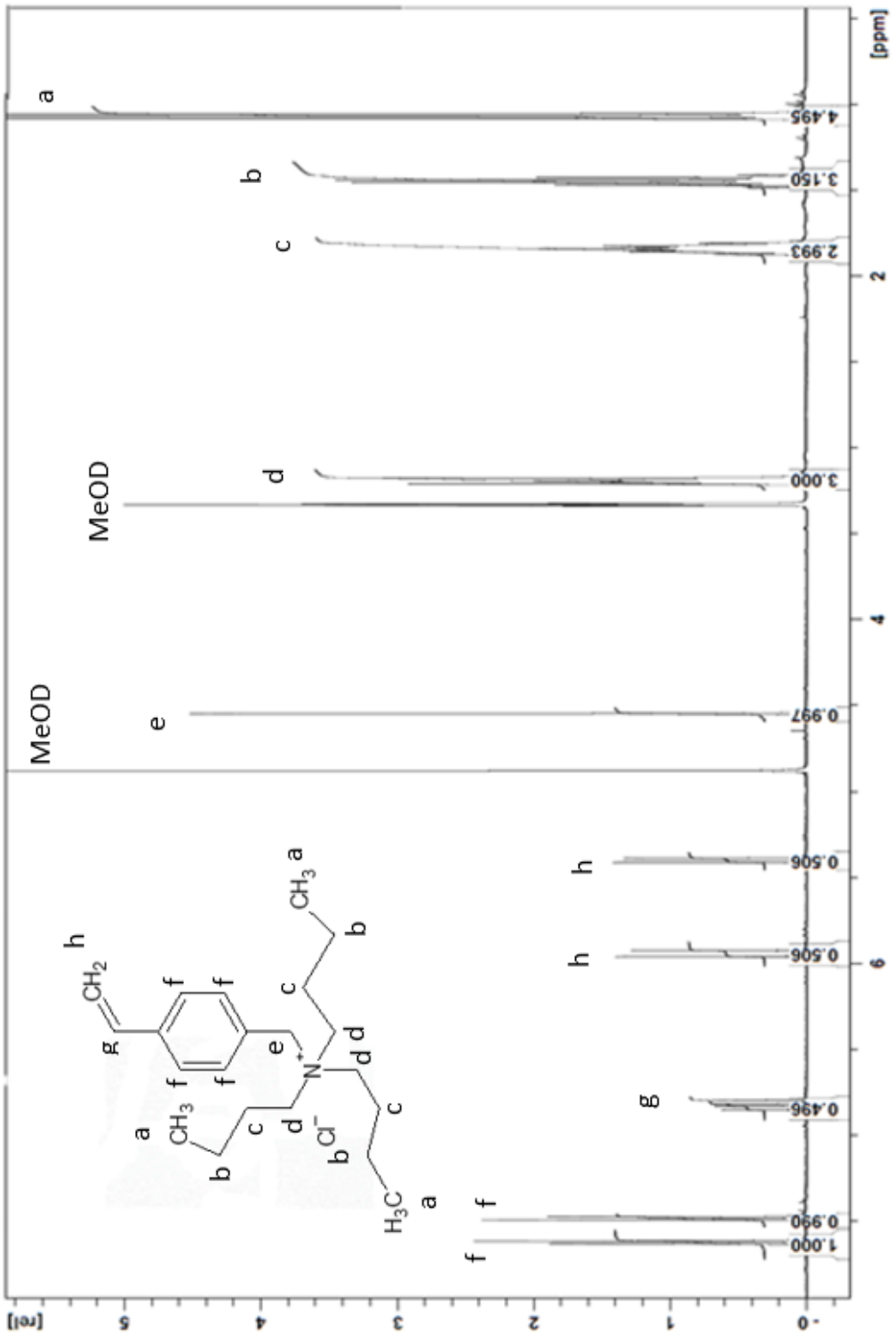

Figure 1. ^{1}H NMR spectrum of the monomer in MeOD.

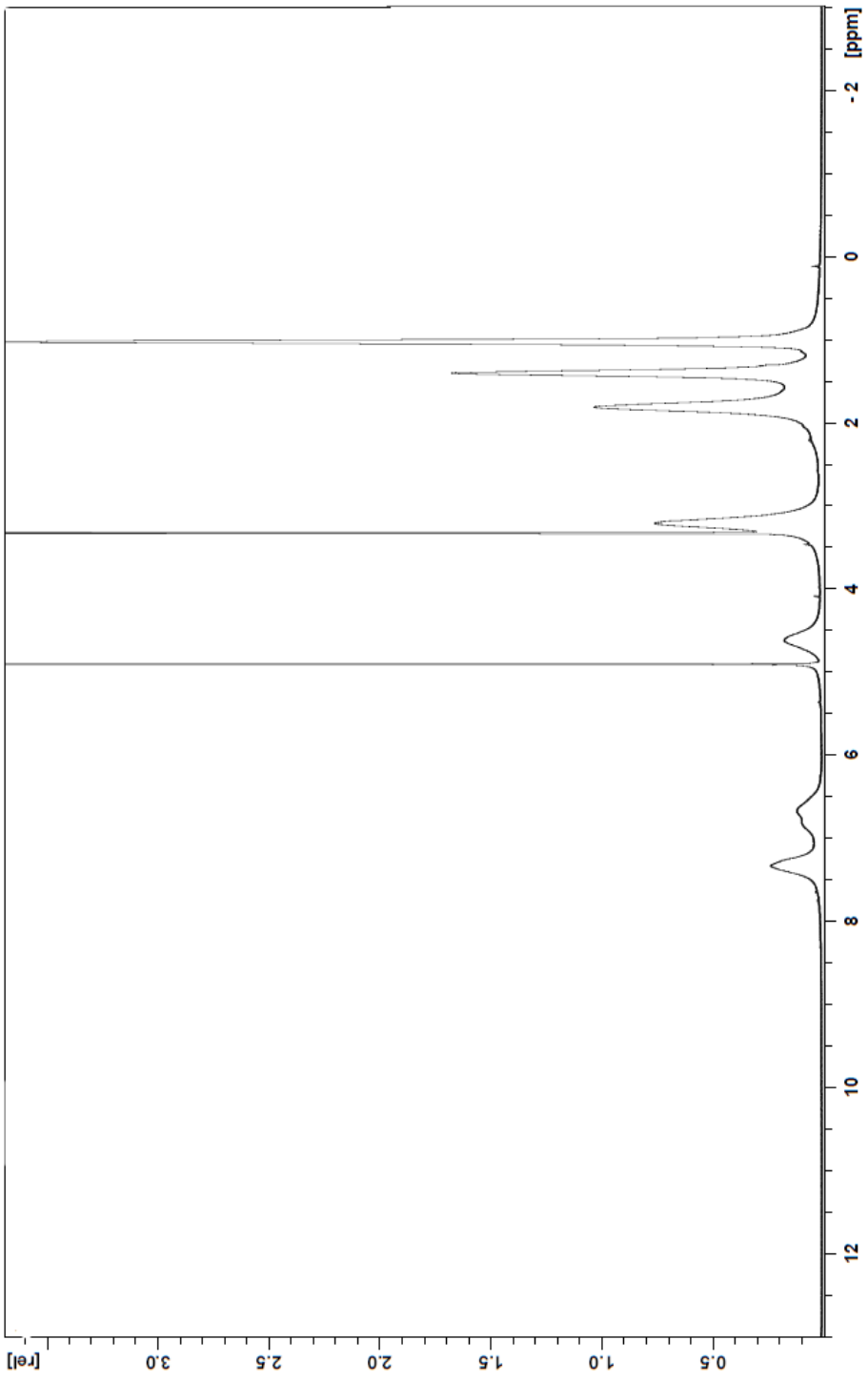

Figure 2. ^{1}H NMR spectrum of the microgel synthesized in NaCl 0.75 M.

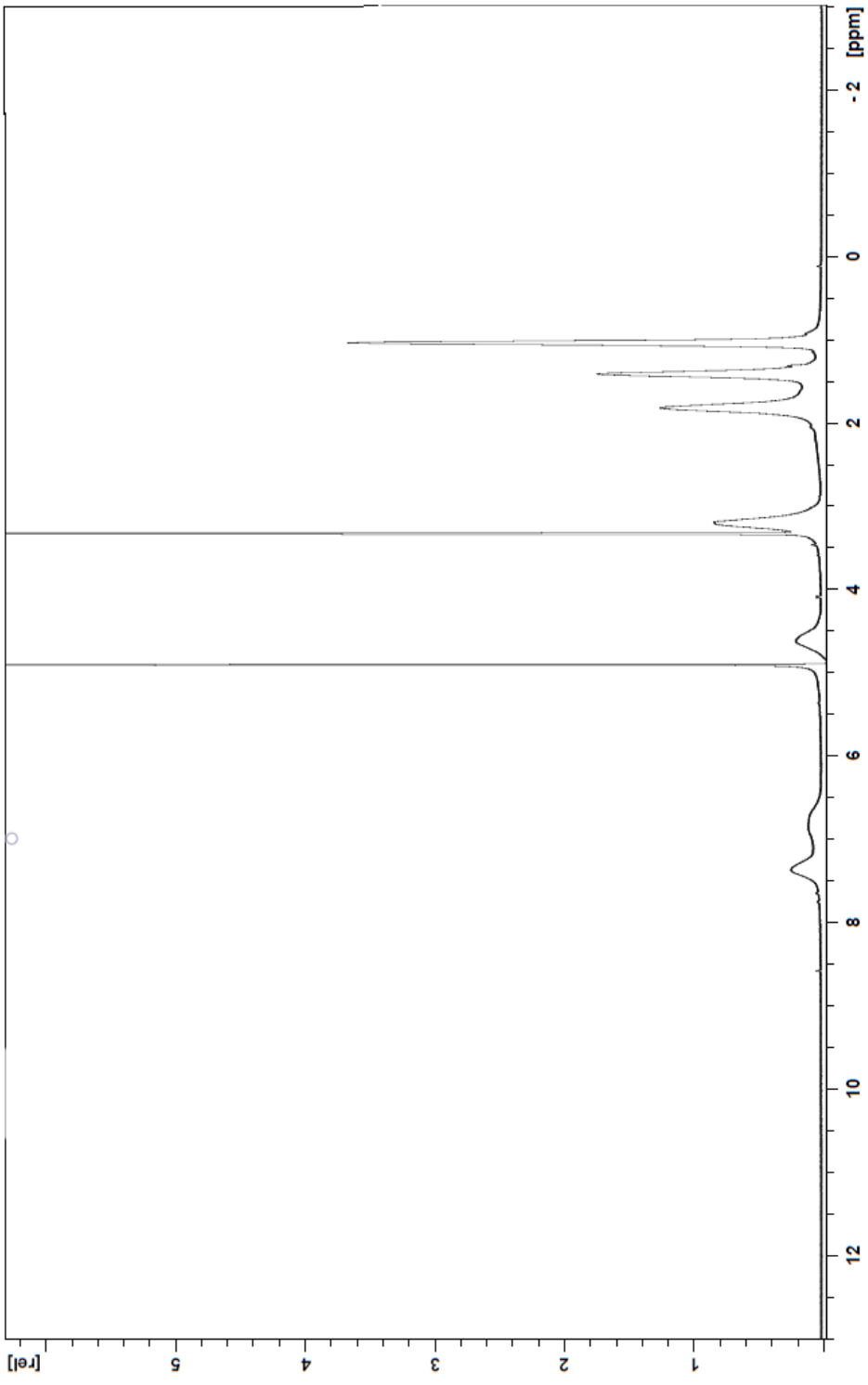

Figure 3. ^{1}H NMR spectrum of the microgel synthesized in DMF 30%.

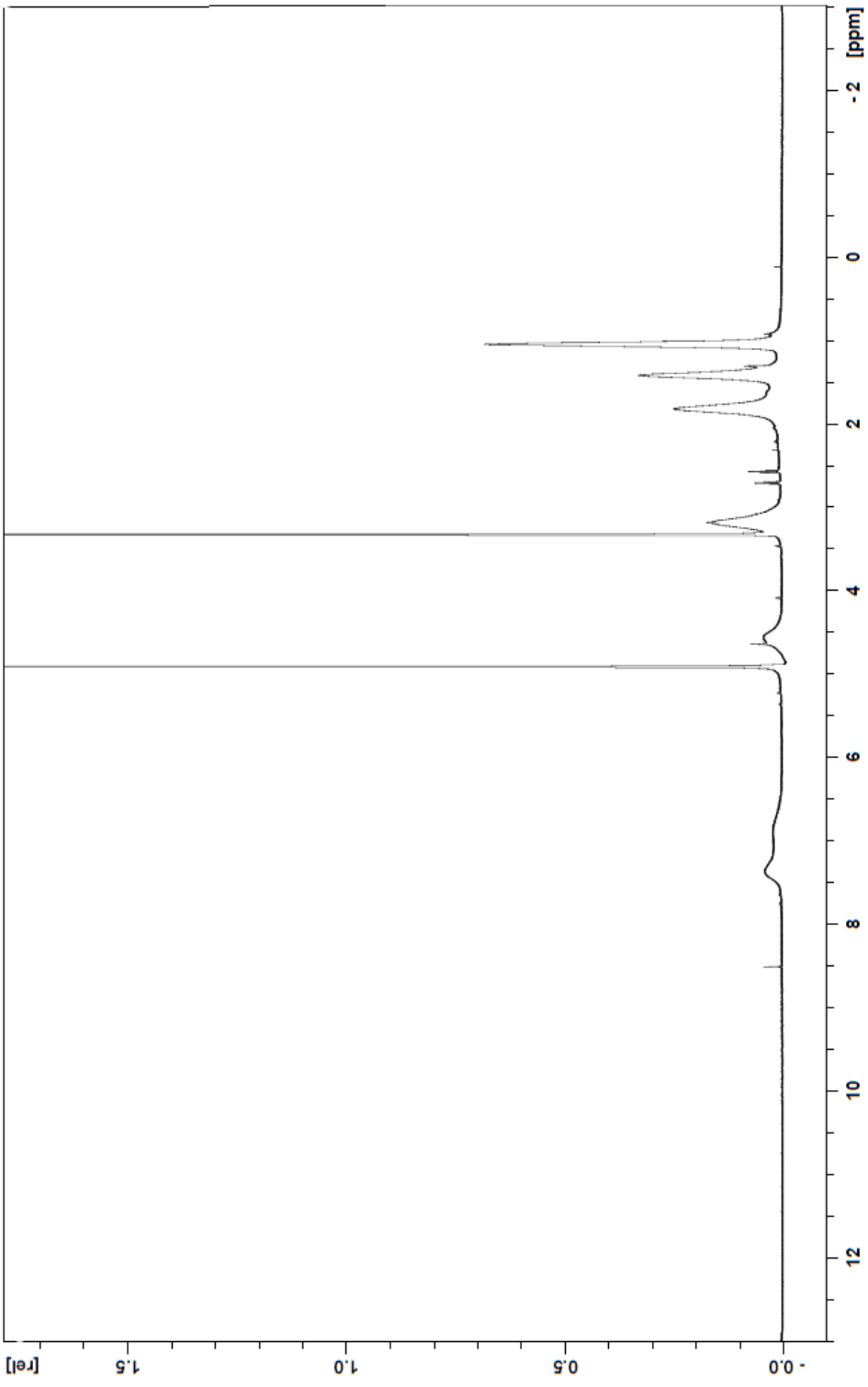

Figure 4. ^{1}H NMR spectrum of the microgel synthesized in DMF 50%.

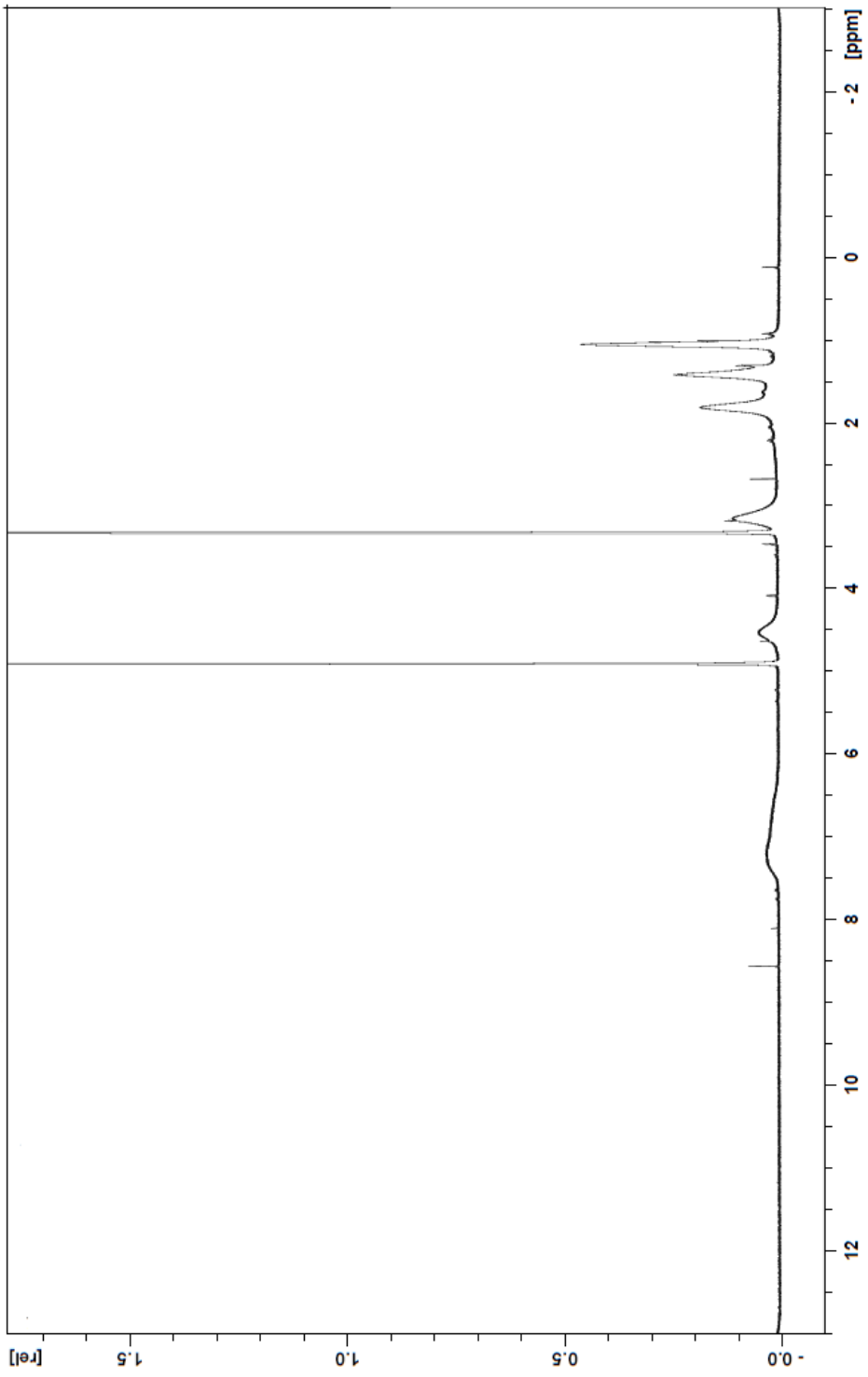

Figure 5. ^{1}H NMR spectrum of the microgel synthesized in DMF 70%.

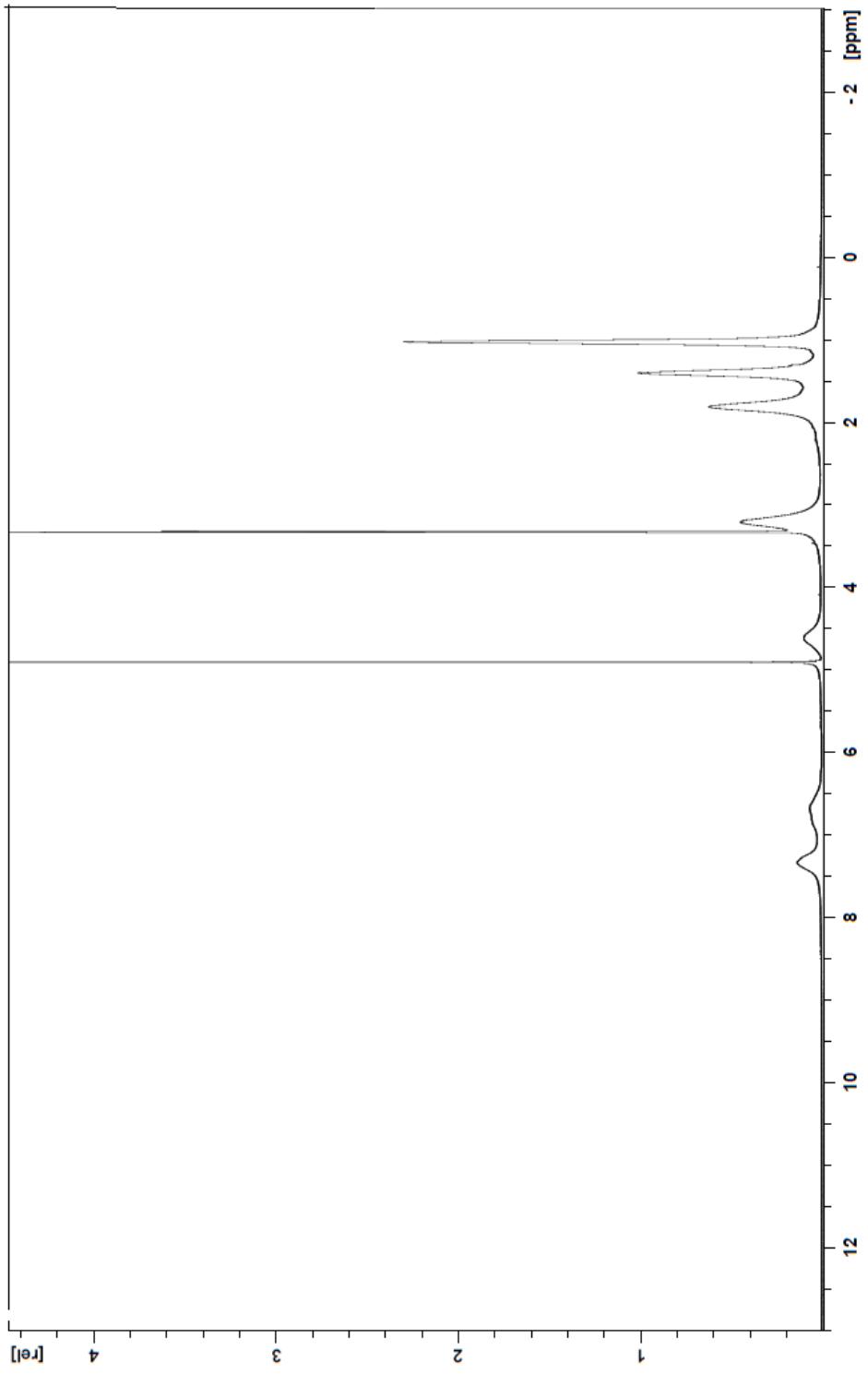

Figure 6. ^{1}H NMR spectrum of the microgel synthesized in DMF 90%.